

Monte Carlo method in nuclear quantum many-body problem

Bing-Nan Lü
呂炳楠

Nuclear Lattice EFT Collaboration



中国工程物理研究院研究生院
GRADUATE SCHOOL OF CHINA ACADEMY OF ENGINEERING PHYSICS



MICHIGAN STATE
UNIVERSITY



中山大學
SUN YAT-SEN UNIVERSITY



OAK RIDGE
National Laboratory
LEADERSHIP COMPUTING FACILITY



Graduate School of China Academy of Engineering Physics Oct-18-2022

量子多体问题的蒙特卡洛方法

吕炳楠



中国工程物理研究院研究生院
GRADUATE SCHOOL OF CHINA ACADEMY OF ENGINEERING PHYSICS

2022年12月17日
2022粒子与核物理理论冬季研讨班-四川大学

报告内容

- 核物理中的量子多体问题
- 量子蒙特卡洛方法
- 格点有效场论及应用

A century of nuclear physics: Where are we now?



Rutherford. Discovery of atomic nucleus. (1908 Nobel Prize)

"Atoms have 99.9% of their mass concentrated in a very small nucleus"



Chadwick. Discovery of neutron. (1935 Nobel Prize)

"Atomic nucleus consists of protons and neutrons"



Yukawa & Powell. Prediction and discovery of pion. (1949 & 1950 Nobel Prize)

"Force pulling nucleons together is mediated by mesons. e.g., pions."



Mayer & Jensen. Nuclear shell model. (1963 Nobel Prize)

"Protons & neutrons in a nucleus move in regular orbits"



A. Bohr & Mottelson & Rainwater. Collective model for nucleus. (1975 Nobel Prize)

"Nucleus can oscillate, rotate, excite and decay, either individually or collectively"



Gell-Mann. Classification of particles. Quark model. (1969 Nobel Prize)

"Proton, neutron and other hadrons are all composite particles composed of quarks"



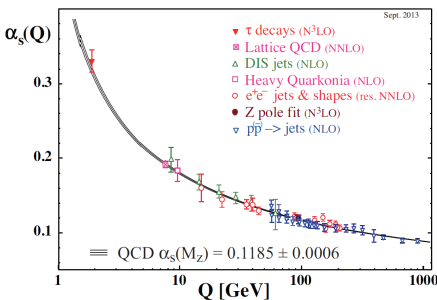
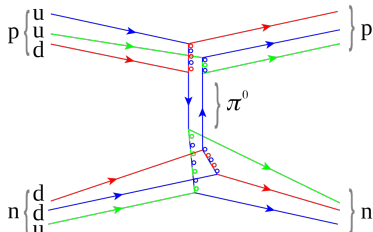
Gross & Politzer & Wilczek. Asymptotic freedom. (2004 Nobel Prize)

"Strong force is weak for high energies. QCD is the correct theory"

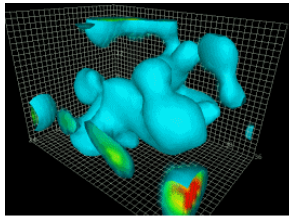
QCD: Fundamental theory of nuclear force

Theory of strong interaction: Quantum Chromodynamics (QCD)

- Quarks: 2 flavors \times 3 colors
- Quark confinement / Asymptotic freedom (**free quarks not seen!**)
- SU(3) gauge field of gluons
- Spontaneously broken chiral symmetry ($M_\pi/M_{\text{proton}} \approx 0.14$,
why pion so light?)
- Yukawa's meson theory is a low energy equivalent



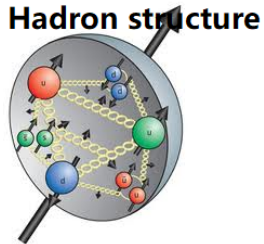
Lattice QCD: First principle, but expensive



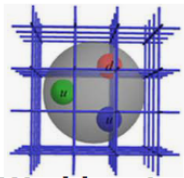
Quarks & Gluons



Supercomputers



Hadron structure



World on Lattice



Stochastic algorithms



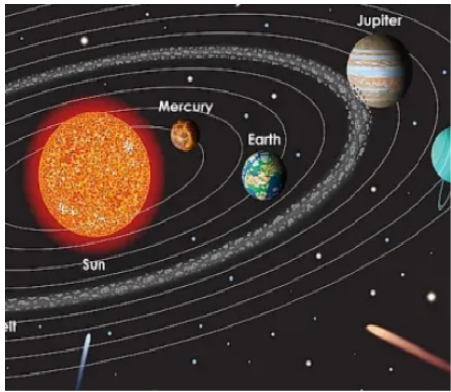
Quantum computing



Démon de Laplace: Given the fundamental laws, we can solve it for everything!

Anonymous Physicist: But every scale has its physics, **more is different!**

Effective theories: Separation of scales



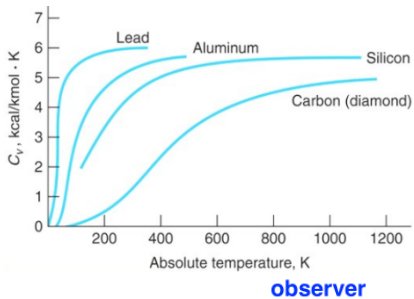
Pale Blue Dot



We can calculate the earth's orbit without knowing the height of the Everest
Everything on the earth are captured in a single parameter, the earth mass M

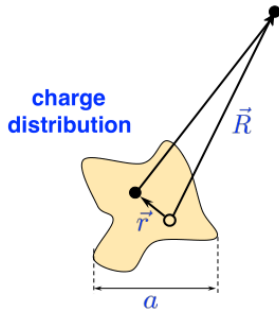
The insight: At astronomical distances, most details of the planets are irrelevant.
They are “renormalized” into a few global parameters.

Frozen degrees of freedom & low energy constants



- Upper panel: Specific heat of solids. At low temperature, most degrees of freedom are frozen.
- Lower panel: At long distances, only the total charge q , dipole moment P_i , quadrupole moment Q_{ij} , ... are important.

$$\begin{aligned}V(\vec{R}) &= \int d^3r \frac{\rho(\vec{r})}{|\vec{R}-\vec{r}|} \\&= \frac{q}{R} + \frac{1}{R^3} \sum_i R_i P_i \\&\quad + \frac{1}{6R^5} \sum_{ij} (3R_i R_j - \delta_{ij} R^2) Q_{ij} + \dots\end{aligned}$$



$$\begin{aligned}q &= \int d^3r \rho(\vec{r}) \\P_i &= \int d^3r \rho(\vec{r}) r_i \\Q_{ij} &= \int d^3r \rho(\vec{r}) (3r_i r_j - \delta_{ij} r^2)\end{aligned}$$

Back to nuclear physics: Separation of scales

Lattice Quantum Chromodynamics

Chiral Effective Field Theory

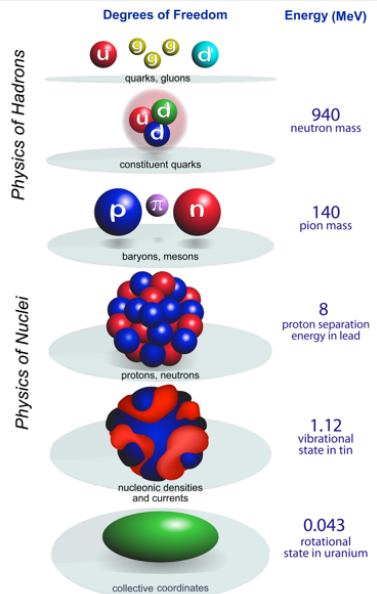
Microscopic A-body Methods

Configuration Interactions

Density Functional Methods

Mean Field Methods

Effective Theory of Collective Modes



W. Nazarewicz

Write down an interaction (fundamentally/effectively)



C. N. Yang, non-Abelian gauge field

"Symmetry dictates interaction"



K. G. Wilson, renormalization group

"Interaction flows with the scale"

We can write a most general Lagrangian for quarks and gluons containing all possible terms
Most of them are excluded by **symmetries** and **renormalizability**

Renormalizable interactions survive when running to low-energies

Non-renormalizable interactions are suppressed when running to low-energies

$$\begin{aligned}\mathcal{L}_{\text{QCD}} = & \sum_{\text{flavors}} \bar{\psi} (i\gamma^\mu \partial_\mu - M) \psi - g A_\mu^i \bar{\psi} \gamma^\mu t_i \psi - \frac{1}{4} G_i^{\mu\nu} G_{\mu\nu}^i \\ & + \frac{1}{2} m_g^2 A_\mu^i A_i^\mu + \frac{1}{2} c \bar{\psi} \sigma^{\mu\nu} t_i \psi G_{\mu\nu}^i + \dots\end{aligned}$$

Suppressed by gauge symmetry Suppressed by renormalizability

Given the **degrees of freedom**, **symmetries** and **energy scales**, we can always construct an effective field theory with the same philosophy.

All theories are EFT. Standard model is an EFT of a quantum gravity theory (string theory?)

The principles for an interaction designer

Weinberg's Folk Theorem:

„if one writes down the most general possible Lagrangian, including all terms consistent with the assumed symmetry principles, and then calculates matrix elements with this Lagrangian to any given order of perturbation theory, the result will simply be the most general possible S-matrix consistent with analyticity, perturbative unitarity, cluster decomposition, and the assumed symmetry properties.“

Physica 96A (1979) 327

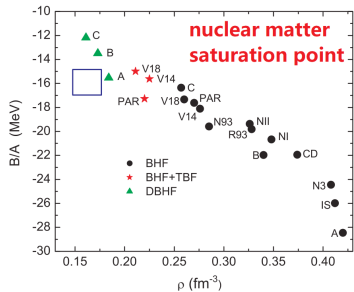
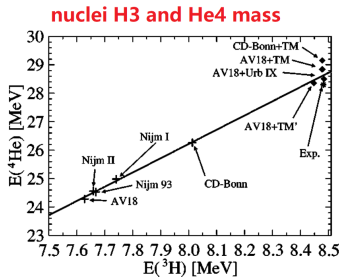
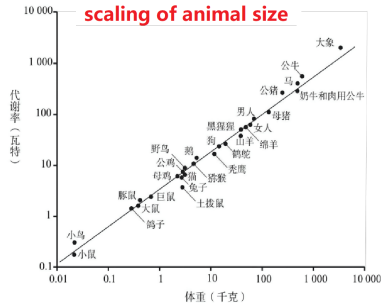
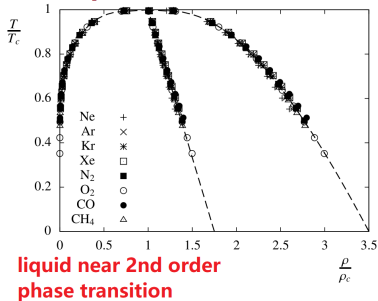
Weinberg's 3rd law of progress in theoretical physics:

„you may use any degrees of freedom you like to describe a physical system, but if you use the wrong ones, you will be sorry.“

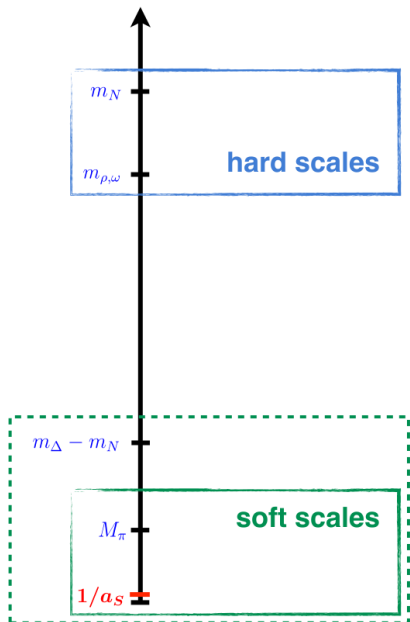
in Asymptotic Realms of Physics, MIT Press, Cambridge, 1983

Universality: Simplicity emerging from Complexity

Universality: Different theories at **small scales** exhibit **unified behaviour** at **large scales**



Scales in chiral EFT

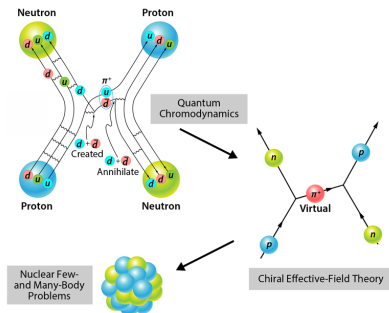


- Chiral EFT: Perturbative expansion of the N - N and π - N potentials in powers of $Q \in \left\{ \frac{M_\pi}{\Lambda}, \frac{|\vec{p}|}{\Lambda} \right\}, \Lambda \sim m_\rho \sim 4\pi F_\pi \sim 1 \text{ GeV}$
- QCD has an approximate chiral symmetry
 - Explicitly broken by non-zero quark mass ($m_q \sim 3 \text{ MeV}$)
 - Spontaneously broken, $SU(2) \times SU(2) \rightarrow SU(2)$
- SB exact symmetry \rightarrow massless Goldstone bosons
- SB approx. symm. \rightarrow very light bosons \rightarrow pions ($M_\pi \sim 140 \text{ MeV}$)
- In nucleus, Fermi momentum $p_F \sim 200 \text{ MeV}$

Chiral effective field theory

Chiral EFT: The low-energy equivalence of the QCD
Weinberg (1979,1990,1991), Gasser, Leutwyler (1984,1985)

- Proton (uud), neutron (udd), pion ($u\bar{d}$)
- Spontaneously broken chiral symmetry:
 $SU(2)_L \times SU(2)_R \rightarrow SU(2)_V$
- Goldstone theorem implies a light pion:
Long-range part of the nuclear force
- Contact terms:
Short-range part of the nuclear force
- Hard scale: $\Lambda_\chi \sim 1 \text{ GeV}$: Chiral EFT works for momentum $Q \ll \Lambda_\chi$



Quarks confined
in nucleons and pions

N - N interaction in nuclear chiral EFT

$$\langle \mathbf{p}'_1, \mathbf{p}'_2 | V_{N-N} | \mathbf{p}_1, \mathbf{p}_2 \rangle = \left\{ B_1 + B_2(\boldsymbol{\sigma}_1 \cdot \boldsymbol{\sigma}_2) + C_1 q^2 + C_2 q^2 (\boldsymbol{\tau}_1 \cdot \boldsymbol{\tau}_2) + C_3 q^2 (\boldsymbol{\sigma}_1 \cdot \boldsymbol{\sigma}_2) + C_4 q^2 (\boldsymbol{\sigma}_1 \cdot \boldsymbol{\sigma}_2)(\boldsymbol{\tau}_1 \cdot \boldsymbol{\tau}_2) \right. \\ + C_5 \frac{i}{2} (\mathbf{q} \times \mathbf{k}) \cdot (\boldsymbol{\sigma}_1 + \boldsymbol{\sigma}_2) + C_6 (\boldsymbol{\sigma}_1 \cdot \mathbf{q})(\boldsymbol{\sigma}_2 \cdot \mathbf{q}) + C_7 (\boldsymbol{\sigma}_1 \cdot \mathbf{q})(\boldsymbol{\sigma}_2 \cdot \mathbf{q})(\boldsymbol{\tau}_1 \cdot \boldsymbol{\tau}_2) \\ \left. - \frac{g_A^2}{4F_\pi^2} \left[\frac{(\boldsymbol{\sigma}_1 \cdot \mathbf{q})(\boldsymbol{\sigma}_2 \cdot \mathbf{q})}{q^2 + M_\pi^2} + C_\pi \boldsymbol{\sigma}_1 \cdot \boldsymbol{\sigma}_2 \right] (\boldsymbol{\tau}_1 \cdot \boldsymbol{\tau}_2) + \dots \right\} \delta(\mathbf{p}_1 + \mathbf{p}_2 - \mathbf{p}'_1 - \mathbf{p}'_2),$$

$\mathbf{q} = \mathbf{p}'_1 - \mathbf{p}_1, \mathbf{k} = \mathbf{p}'_2 - \mathbf{p}_2, \boldsymbol{\sigma}_{1,2}$ for spins, $\boldsymbol{\tau}_{1,2}$ for isospins, C_{1-7} , g_A , etc. are Low Energy Constants fitted to N - N scattering data

	Two-nucleon force	Three-nucleon force	Four-nucleon force
$\mathcal{O}((Q/\Lambda_\chi)^0)$	X H	—	—
	2 LECs		
$\mathcal{O}((Q/\Lambda_\chi)^2)$	X e K H	—	—
	7 LECs		
$\mathcal{O}((Q/\Lambda_\chi)^3)$	H K	X X *	—
	2 LECs		
$\mathcal{O}((Q/\Lambda_\chi)^4)$	X e K H ...	K H K X ...	H H H H ...
	15 LECs		

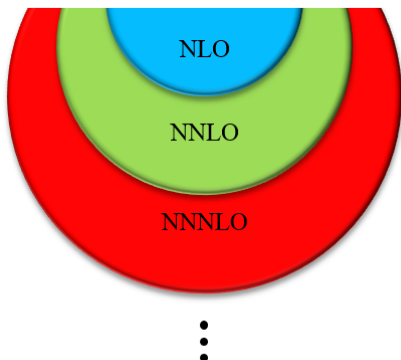
Strategy for a practical calculation

Non-perturbative – Monte Carlo



“Improved LO”

Perturbative corrections

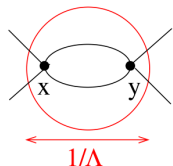


Mysterious three-body force: An EFT view

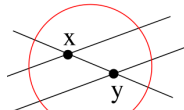
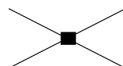
Three-body force emerges when short-range correlations are integrated out

Peculiarities in three-body systems: **Thomas collapse**, **Efimov physics**, **Borromean state**, ...

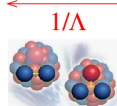
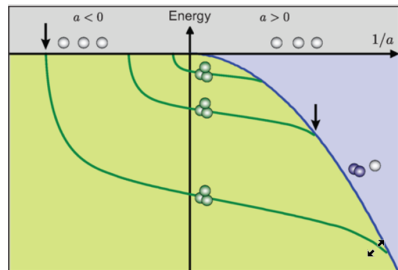
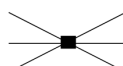
Three-body forces are difficult to fix. Still not fully understood in modern nuclear theories



+ ...



+ ...



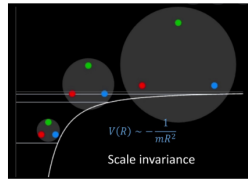
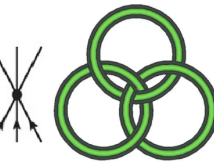
A



B



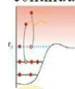
C



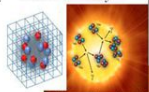
Hot Topics in Nuclear Physics

*Physics at
the Femtometer scale*

Coupling to
continuum



Lattice Effective Field Theory

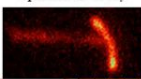


E
L
H
H

P_v

Neutron halos

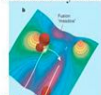
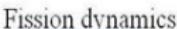
2p radioactivity



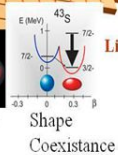
V- π pairing



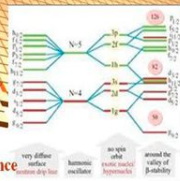
Equation of state



Voyage to
SUPERHEAVY Island

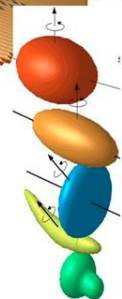


Coexistence



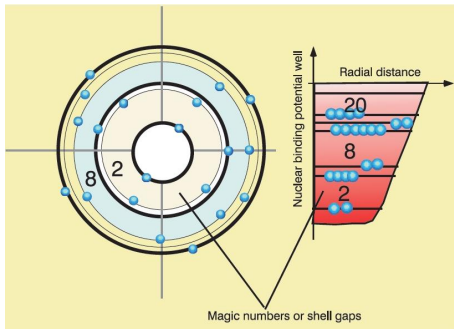
New magic numbers

Exotic Shapes



Introduction: Standard model of nuclear physics

- Shell model: mean field, shell structure, no central force (M. Mayer, J. Jensen, 1963 Nobel Prize)



- Collective motions: rotation and vibration, particle-vibration coupling (A. Bohr, B. Mottelson, J. Rainwater, 1975 Nobel Prize)



Introduction: Modern nuclear theories

Road map - Towards a comprehensive description of the nucleus

- ***Ab initio* methods:**

- Microscopic interactions

- Lattice QCD ($A = 0, 1, 2, \dots$)

- NCSM, F-Y, GFMC ($A = 3-16$)

- Coupled cluster, IMSRG ($A = 16-100$)

- **Configuration-interaction theories:**

- Phenomenological interactions

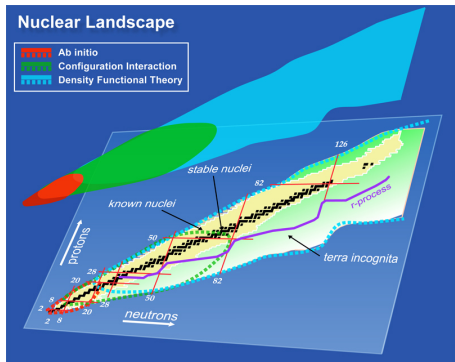
- Shell model

- **Density functional theories:**

- Phenomenological interactions

- mean field approximation

- Skyrme, Gogny, RMF, ...



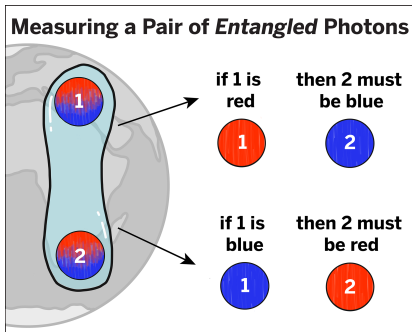
Lattice EFT: *Ab initio* method for $A = 3-100$

Why need nuclear ab initio methods

Mean field models are useful

but **quantum correlations** not included

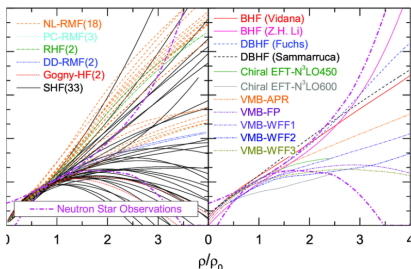
$$|\Psi\rangle = 1/\sqrt{2} [|0\rangle|1\rangle + |1\rangle|0\rangle]$$



In mean field models, motion of particle 1
is independent of other particles
 $P(1,2) = P(1) \times P(2)$

Predictions are **model-dependent**

Example: symmetry energy



N.-B. Zhang and B.-A. Li, EPJA 55, 39 (2019)

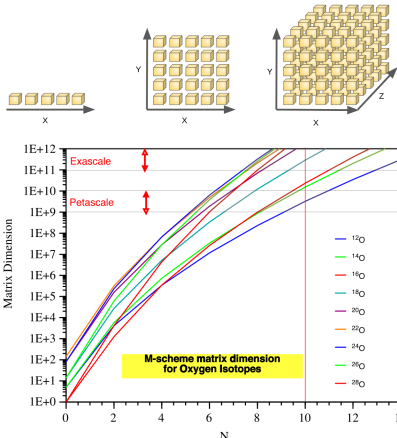
Symptom 1: Lack of quantum correlations

Symptom 2: Imprecise nuclear forces

Recipe: Exactly solve many-body Schrödinger equation with precise nuclear force \implies **nuclear ab initio methods**

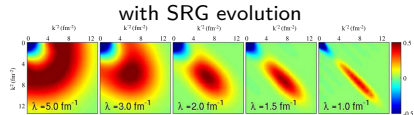
Dimensionality curse in nuclear many-body problems

Exponential increase of resources



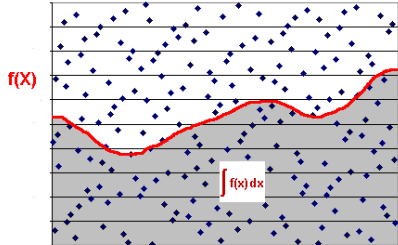
PRC 101, 014318 (2020)

Solution 1: Reduce effective Hilbert space



Solution 2: Monte Carlo algorithms

The Monte Carlo Integral

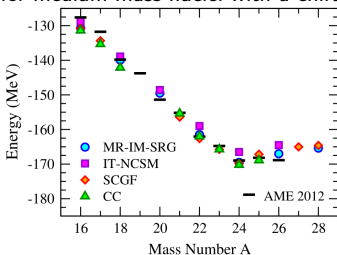


Benchmark for *ab initio* methods

Benchmark for ^4He with a AV8' NN interaction

Method	$\langle T \rangle$	$\langle V \rangle$	E_b	$\sqrt{\langle r^2 \rangle}$
FY	102.39(5)	-128.33(10)	-25.94(5)	1.485(3)
CRCGV	102.30	-128.20	-25.90	1.482
SVM	102.35	-128.27	-25.92	1.486
HH	102.44	-128.34	-25.90(1)	1.483
GFMC	102.3(1.0)	-128.25(1.0)	-25.93(2)	1.490(5)
NCSM	103.35	-129.45	-25.80(20)	1.485
EIHH	100.8(9)	-126.7(9)	-25.944(10)	1.486

Benchmark for medium mass nuclei with a chiral interaction



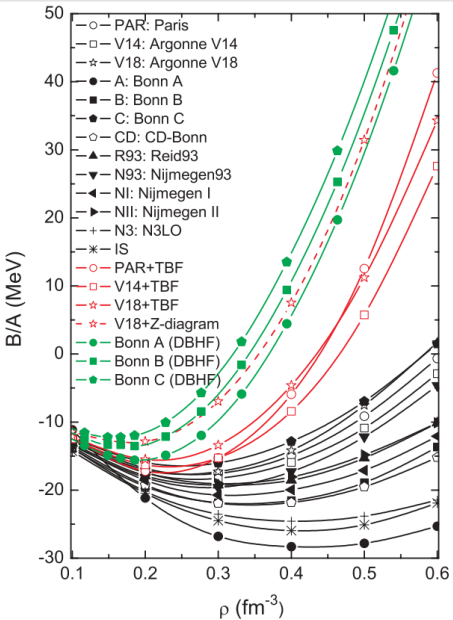
PRC 64, 044001 (2001); Annu. Rev. Nucl. Part. Sci. 65, 457 (2015)

Introduction: A puzzle in nuclear forces

- High precision nuclear forces are constrained by the **Low-energy Nucleon-Nucleon scattering data**
- Quite **different predictions for nuclear matter and medium mass nuclei**
- **Fails** to reproduce the binding energies and/or charge radii globally
- **Example:** Energy vs. Density for homogenous nuclear matter

Question: What are the **essential elements** for the nuclear binding?

Requires efficient many-body methods!

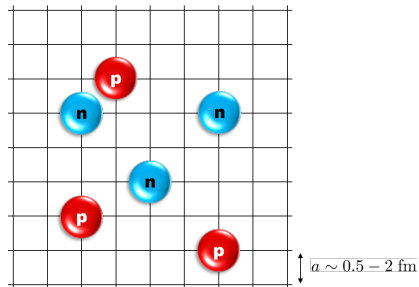


Introduction to Lattice Effective Field Theory

Lattice EFT = Chiral EFT + Lattice + Monte Carlo

Review: Dean Lee, Prog. Part. Nucl. Phys. 63, 117 (2009),
Lähde, Meißner, "Nuclear Lattice Effective Field Theory", Springer (2019)

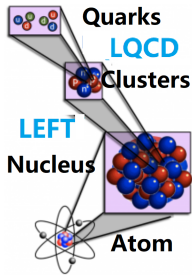
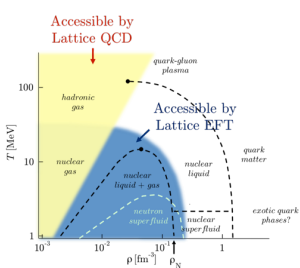
- Discretized **chiral nuclear force**
- Lattice spacing $a \approx 1 \text{ fm} = 620 \text{ MeV}$
(\sim chiral symmetry breaking scale)
- Protons & neutrons interacting via
short-range, δ -like and **long-range,**
pion-exchange interactions
- Exact method, **polynomial scaling** ($\sim A^2$)



Lattice adapted for nucleus

Comparison to Lattice QCD

	LQCD	LEFT
degree of freedom	quarks & gluons	nucleons and pions
lattice spacing	$\sim 0.1 \text{ fm}$	$\sim 1 \text{ fm}$
dispersion relation	relativistic	non-relativistic
renormalizability	renormalizable	effective field theory
continuum limit	yes	no
Coulomb	difficult	easy
accessibility	high T / low ρ	low T / ρ_{sat}
sign problem	severe for $\mu > 0$	moderate



Euclidean time projection

- Get interacting g. s. from imaginary time projection:

$$|\Psi_{g.s.}\rangle \propto \lim_{\tau \rightarrow \infty} \exp(-\tau H) |\Psi_A\rangle$$

with $|\Psi_A\rangle$ representing A free nucleons.

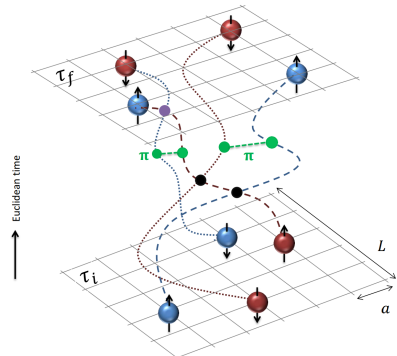
- Expectation value of any operator \mathcal{O} :

$$\langle \mathcal{O} \rangle = \lim_{\tau \rightarrow \infty} \frac{\langle \Psi_A | \exp(-\tau H/2) \mathcal{O} \exp(-\tau H/2) | \Psi_A \rangle}{\langle \Psi_A | \exp(-\tau H) | \Psi_A \rangle}$$

- τ is discretized into time slices:

$$\exp(-\tau H) \simeq \left[: \exp\left(-\frac{\tau}{L_t} H\right) : \right]^{L_t}$$

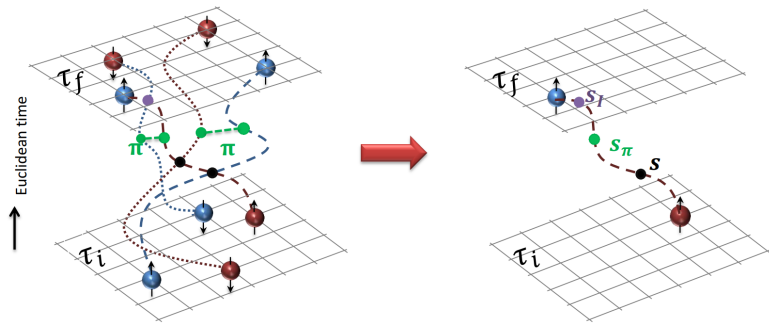
All possible configurations in $\tau \in [\tau_i, \tau_f]$ are sampled.
Complex structures like nucleon clustering emerges naturally.



Auxiliary field transformation

Quantum correlations between nucleons are represented by fluctuations of the auxiliary fields.

$$:\exp\left[-\frac{C}{2}(N^\dagger N)^2\right]:= \frac{1}{\sqrt{2\pi}} \int ds :\exp\left[-\frac{s^2}{2} + \sqrt{C}s(N^\dagger N)\right]:$$



Imaginary time extrapolation to find ground state

Samples are generated by
Markov Chain Monte Carlo

Observables calculated as $\langle O \rangle = (1/N) \sum_{i=1}^N O_i$

Error scales as $\varepsilon \sim \mathcal{O}(1/\sqrt{N})$

Number of samples $N \sim 10^3 \sim 10^6$

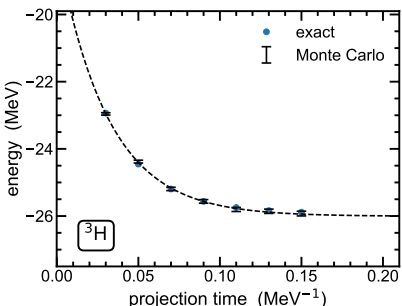
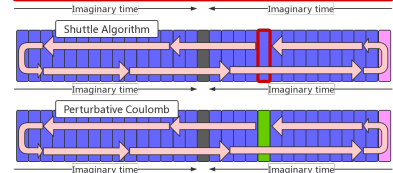
Total energies at large t follow

$$E_A(t) = E_A(\infty) + c \exp[-\Delta E t].$$

For any inserted operator \mathcal{O} ,

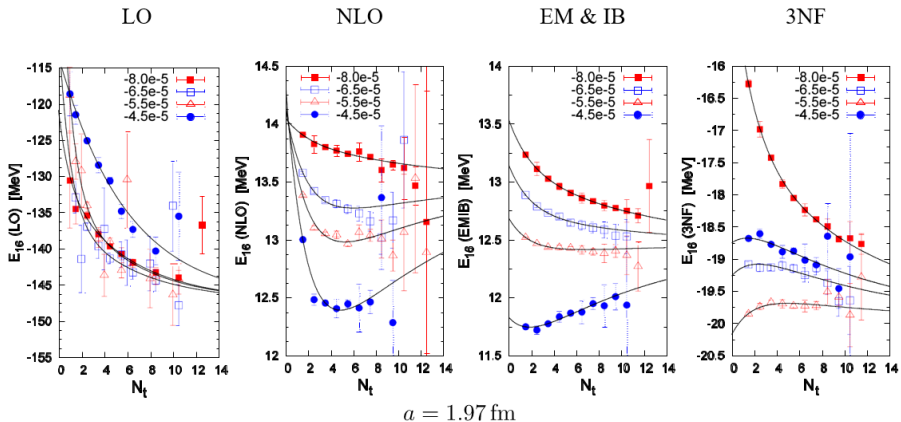
$$\mathcal{O}_A(t) = \mathcal{O}_A(\infty) + c' \exp[-\Delta E t/2],$$

$c, c', \Delta E$ are **fitting parameters**.



A real lattice EFT calculation

Oxygen-16 ground state



Epelbaum, Krebs, Lähde, D.L, Meißner, Rupak, PRL112, 102501 (2014)

Introduction to Monte Carlo techniques

Consider approximating a one-dimensional integral by a simple Riemann sum

$$I = \int_0^L dx f(x) \approx \frac{L}{N} \sum_{j=1}^N f(x^{(j)})$$

The x_i 's are at regularly spaced intervals.

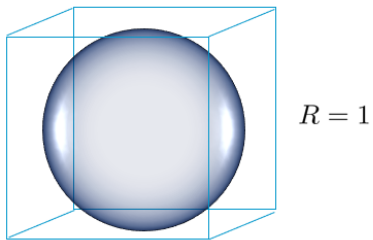
Generalization to d dimensions is more challenging. If we keep the same number of grid points, N , then only $N^{1/d}$ points per dimension and relative error can be quite large.

$$\begin{aligned} I &= \int_0^L dx_1 \cdots \int_0^L dx_d f(x_1, \dots, x_d) \\ &\approx \frac{L^d}{N} \sum_{j_1=1}^{N^{1/d}} \cdots \sum_{j_d=1}^{N^{1/d}} f(x_1^{(j_1)}, \dots, x_d^{(j_d)}) \end{aligned}$$

Introduction to Monte Carlo techniques

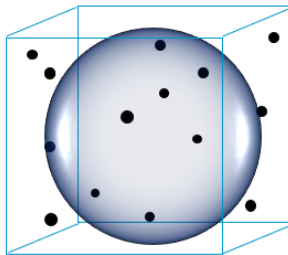
Suppose instead we choose the points at random positions in the d -dimensional space. Then relative error is purely statistical and can be as small as $N^{-1/2}$

Example: Volume of 3D sphere using random darts



$$\frac{4\pi}{3} = \int_{-1}^1 \int_{-1}^1 \int_{-1}^1 dx dy dz \theta(1 - x^2 - y^2 - z^2)$$

Introduction to Monte Carlo techniques



Select N uniformly distributed random points inside the cube. Determine the fraction of points inside the sphere. This gives an estimate for the ratio of the sphere volume to cube volume.

$$\frac{4\pi}{3} = V_{\text{cube}} \frac{V_{\text{sphere}}}{V_{\text{cube}}}$$

$$\approx 8 \cdot \frac{1}{N} \sum_{i=1}^N \theta \left[1 - (x^{(i)})^2 - (y^{(i)})^2 - (z^{(i)})^2 \right]$$

Introduction to Monte Carlo techniques

When calculating thermal averages in statistical mechanics or path integrals in Euclidean-time field theory, one computes sums or integrals over many degrees of freedom weighted by an exponential Boltzmann factor

$$\langle M \rangle = \frac{\sum_C M(C) e^{-\beta E(C)}}{\sum_C e^{-\beta E(C)}}$$

Due to the exponential weight, nearly all of the configurations make only a very small contribution. So a simple dartboard random sampling is very inefficient.

Importance sampling

A more efficient method to calculate the average is to select configurations with probability equal to

Introduction to Monte Carlo techniques

$$p_\beta(C) = \frac{e^{-\beta E(C)}}{\sum_{C'} e^{-\beta E(C')}}$$

This technique is called importance sampling. The thermal average is simply an average over representative configurations selected with this sampling probability.

$$\langle M \rangle = \frac{1}{N} \sum_j M(C^{(j)})$$

The next step is to devise a way to select configurations with this sampling probability.

Introduction to Monte Carlo techniques

We outline the ingredients of a Markov process. Consider a chain of configurations labeled by order of selection. We call this integer-valued label the computation step, τ .

Let us denote the probability of selecting configuration A at computation step τ as

$$P(A, \tau)$$

Suppose we have selected configuration A at computation step τ . The probability that we select configuration B at computation step $\tau + 1$ is denoted

$$W(A \rightarrow B)$$

Introduction to Monte Carlo techniques

This transition probability is independent of τ and independent of the history of configurations selected prior to selecting A at computation step τ . This defines a Markov process.

We note that

$$\begin{aligned} P(A, \tau + 1) &= P(A, \tau) + \sum_{B \neq A} W(B \rightarrow A)P(B, \tau) \\ &\quad - \sum_{B \neq A} W(A \rightarrow B)P(A, \tau) \end{aligned}$$

If the Markov process is ergodic, then after many computation steps, an equilibrium probability distribution is reached

$$\lim_{\tau \rightarrow \infty} P(C, \tau) \rightarrow p(C)$$

Introduction to Monte Carlo techniques

Detailed balance

We want the equilibrium probability distribution to be

$$p_\beta(C) = \frac{e^{-\beta E(C)}}{\sum_{C'} e^{-\beta E(C')}}$$

One way to do this is to require

$$W(A \rightarrow B)p_\beta(A) = W(B \rightarrow A)p_\beta(B)$$

for every pair of configurations A and B . This condition is called detailed balance.

After many computation steps we reach the equilibrium distribution, which satisfies

$$\sum_{B \neq A} W(A \rightarrow B)p(A) = \sum_{B \neq A} W(B \rightarrow A)p(B)$$

Introduction to Monte Carlo techniques

Comparing with the detailed balance condition, we conclude that

$$p(A) = p_\beta(A)$$

for all configurations A .

Metropolis algorithm

One popular method for generating the desired detailed balance condition is the Metropolis algorithm

Metropolis, Teller, Rosenbluth, J. Chem. Phys. 21 (1953) 1087

$$W(A \rightarrow B) = \begin{cases} e^{-\beta[E(B)-E(A)]} & E(B) > E(A) \\ 1 & E(B) \leq E(A) \end{cases}$$

Introduction to Monte Carlo techniques

Once your Markov chain is set up properly, you can now compute observables such as

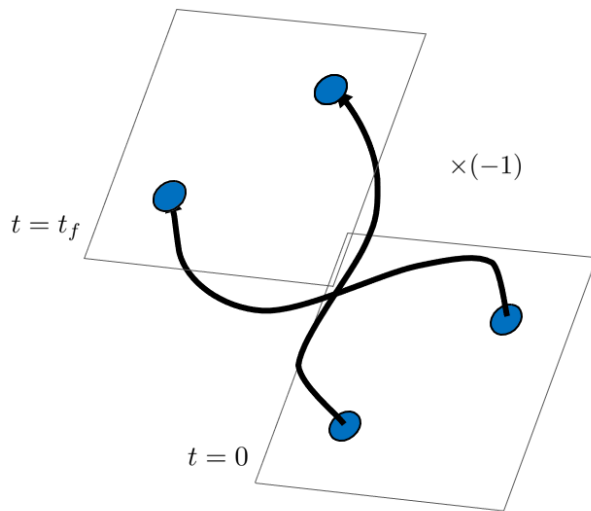
$$\langle O \rangle = \frac{\sum_A O(A) p_{\text{target}}(A)}{\sum_A p_{\text{target}}(A)}$$

by computing the average

$$\langle O \rangle = \frac{\sum_{n=1, N} O(A_n)}{N}$$

for large N from your Markov chain.

Introduction to Monte Carlo techniques



Interchange of two identical fermions produces a minus sign in the path integral

Introduction to Monte Carlo techniques

This results in the fermion sign problem. The final result for the path integral is very small due to sign cancellations. The level of cancellations is given by

$$\langle \text{sign}(C) \rangle \sim \exp [- (E_0^{\text{fermionic}} - E_0^{\text{bosonic}}) t_f]$$

This can be extremely severe. Analogous to calculating the number 1 by evaluating each term in the binomial expansion

$$1 = (2 - 1)^{1000} = 2^{1000} - 1000 \cdot 2^{999} 1^1 + \dots$$

Usually some additional constraint such as the fixed-node approximation or constraint on worldlines is needed.

Introduction to Monte Carlo techniques

$$Z_{n_t, \text{LO}} = \langle \psi_{\text{init}} | \text{[Diagram]} | \psi_{\text{init}} \rangle$$

For simplicity we discuss the structure of the LO₁ and LO₂ calculations

$$Z_{n_t, \text{LO}} = \det \mathbf{M}(s, s_I, \pi_I)$$

$$\mathbf{M}_{ij}(s, s_I, \pi_I) = \langle \vec{p}_i | M^{(L_t-1)}(s, s_I, \pi_I) \cdots M^{(0)}(s, s_I, \pi_I) | \vec{p}_j \rangle$$

For A nucleons, the matrix is A by A . If there is no pion coupling and the quantum state has total isospin equal to zero then

$$\tau_2 \vec{\tau} \tau_2 = -\vec{\tau}^*$$

$$\tau_2 \mathbf{M} \tau_2 = \mathbf{M}^*$$

Introduction to Monte Carlo techniques

This shows the determinant is real. Actually we can show that the determinant is positive semi-definite. Consider an eigenvector

$$\mathbf{M}\phi = \lambda\phi$$

Let us define a new vector

$$\tilde{\phi} = \tau_2\phi^*$$

Note that

$$\begin{aligned}\mathbf{M}\tilde{\phi} &= \mathbf{M}\tau_2\phi^* = \tau_2\tau_2\mathbf{M}\phi^* = \tau_2\mathbf{M}^*\phi^* \\ &= \tau_2(\mathbf{M}\phi)^* = \tau_2(\lambda\phi)^* = \lambda^*\tau_2\phi^* = \lambda^*\tilde{\phi}\end{aligned}$$

Note also that the two vectors are orthogonal

$$\tilde{\phi}^\dagger\phi = (\tau_2\phi^*)^\dagger\phi = \phi^T\tau_2^\dagger\phi = \phi^T\tau_2\phi = 0$$

So the complex eigenvalues come in conjugate pairs, and the real spectrum is doubly-degenerate.

Introduction to Monte Carlo techniques

Let

$$M = \begin{bmatrix} 1.1 & 0.1 & 0.1 \\ 0.1 & 0.8 & 0.1 \\ 0.1 & 0.1 & 0.8 \end{bmatrix} \quad f(n) = [1 \ 0 \ 0] M^n \begin{bmatrix} 1 \\ 0 \\ 0 \end{bmatrix}$$

Construct a Markov process with the Metropolis algorithm to compute

$$f(20)/f(19)$$

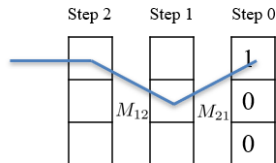
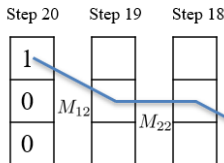
by sampling over all terms in the matrix product

$$[1 \ 0 \ 0] M \cdot M \cdot \dots \cdot M \begin{bmatrix} 1 \\ 0 \\ 0 \end{bmatrix}$$

Introduction to Monte Carlo techniques

Consider any product of matrix elements which contributes to $f(20)$

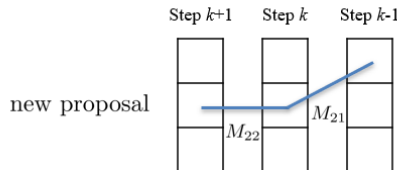
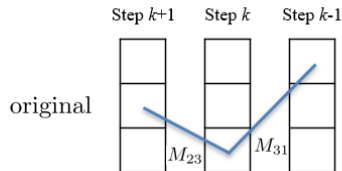
$$M_{12}M_{22} \cdots M_{12}M_{21}$$



Let $W^{(20)}(M_{12}, M_{22}, \dots, M_{12}, M_{21}) = M_{12}M_{22} \cdots M_{12}M_{21}$ be the relative weight for this 20-step path configuration. $W^{(20)}$ is the equivalent of $\exp[-\beta E(C)]$.

For the configuration updates, consider changing the state at step k .

Introduction to Monte Carlo techniques



Ratio of relative weights is

$$\frac{W^{(20)}(\text{new})}{W^{(20)}(\text{original})} = \frac{M_{22}M_{21}}{M_{23}M_{31}}$$

Introduction to Monte Carlo techniques

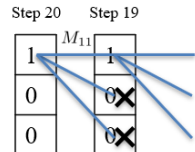
Pick r , a random number between 0 and 1. If

$$r \leq \frac{W^{(20)}(\text{new})}{W^{(20)}(\text{original})}$$

then accept the new update. Otherwise go back to the original. As you sample the 20-step paths you also keep track of the 19-step path weight $W^{(19)}$.

If the row position at step 19 is $j = 1, 2, 3$ then

$$\frac{W^{(19)}}{W^{(20)}} = \begin{cases} \frac{1}{M_{11}} & \text{for } j = 1 \\ 0 & \text{for } j = 2, 3 \end{cases}$$



You average $\frac{W^{(19)}}{W^{(20)}}$ over all 20-step path configurations.

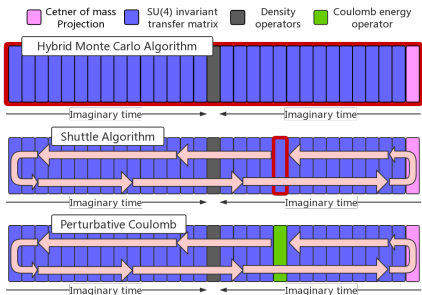
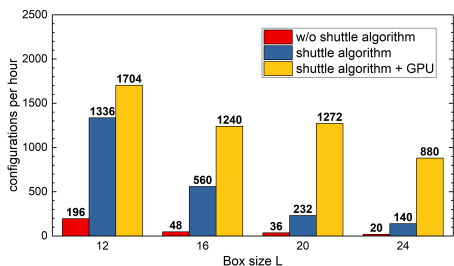
Advanced algorithm and programming paradigm

All $L_t \times L^3$ auxiliary fields s_{n,n_t} need to be updated. Two algorithms:

- Update all fields once every iteration: **Hybrid Monte Carlo**
- Update a single time slice every iteration: **Shuttle Algorithm**

B.L., et. al., PLB 797, 134863 (2019)

SA 5~10 times faster than HMC



- Can be implemented for GPU
- **Algorithm & Hardware** combined give a **40~50 times** speed-up

Large lattices are accessible

Chiral nuclear force on the lattice

Borasoy et al., Eur. Phys. J. A 34(2007) 185

Carlson et al., Nucl. Phys. A 424 (1984) 47

Lu et al., Phys. Lett. B 760 (2016) 309

Kinetic energy term on the lattice

These are defined to give a quadratic kinetic energy as function of momentum

$$\omega_0 - \omega_1 \cos q_l + \omega_2 \cos 2q_l - \omega_3 \cos 3q_l + \dots = \frac{q_l^2}{2} [1 + O(q_l^{2\nu+2})]$$

2ν is the order of lattice improvement for the kinetic energy

$$O(a^0) : \omega_0 = 1, \quad \omega_1 = 1, \quad \omega_2 = 0, \quad \omega_3 = 0$$

$$O(a^2) : \omega_0 = \frac{5}{4}, \quad \omega_1 = \frac{4}{3}, \quad \omega_2 = \frac{1}{12}, \quad \omega_3 = 0$$

$$O(a^4) : \omega_0 = \frac{49}{36}, \quad \omega_1 = \frac{3}{2}, \quad \omega_2 = \frac{3}{20}, \quad \omega_3 = \frac{1}{90}$$

Partial wave analysis of N-N scattering

The radial Schrödinger equation gives

$$\left\{ -\frac{1}{2\mu} \frac{d}{dr} \left(r^2 \frac{d}{dr} \right) + \frac{\ell(\ell+1)}{2\mu r^2} + V(r) \right\} R(r) = E R(r)$$

$$u(r) = r R(r)$$

$$-\frac{1}{2\mu} \frac{d^2 u}{dr^2} + \left[\frac{\ell(\ell+1)}{2\mu r^2} + V(r) \right] u(r) = E u(r)$$

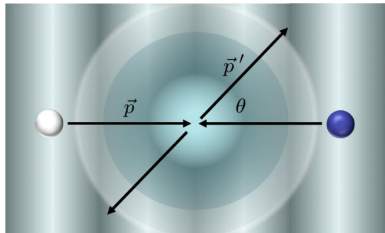
Beyond the range of the interaction, the wave function has the form

$$R(r) \propto \cos \delta_\ell j_\ell(kr) - \sin \delta_\ell y_\ell(kr)$$

N-N scattering in the center of mass frame

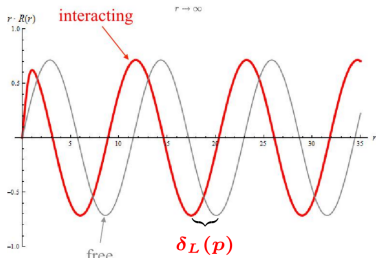
For scattering in the **continuum**:

- Partial wave expansion:
 $\psi(\vec{r}) = \sum_{J=0}^{\infty} \psi_J(r) P_J(\cos \theta)$
- Asymptotically ($r > R_{\text{force}}$):
 $\psi_J(r) \rightarrow A h_J^+(kr) - B h_J^-(kr)$
- Phase shift: $e^{2i\delta} = B/A$



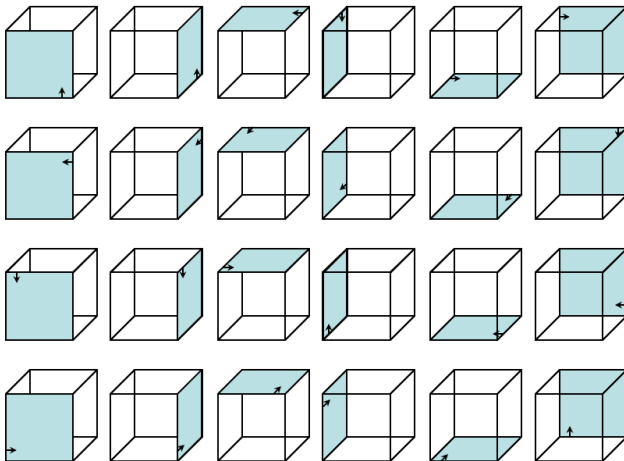
For scattering in a **finite volume**:

- Luescher's formula:
$$e^{2i\delta} = \frac{Z_{00}(1;q^2) + i\pi^{3/2}q}{Z_{00}(1;q^2) - i\pi^{3/2}q}, \quad q = \frac{2\pi n}{L}$$
$$Z_{00}(s, q^2) = \frac{1}{\sqrt{4\pi}} \sum_n \frac{1}{(n^2 - q^2)^s}$$
- Standard tool in LQCD
[Beane et al., Int. J. Mod. Phys. E 17\(2008\) 1517](#)
- Not applicable in LEFT: noisy data, need higher precision

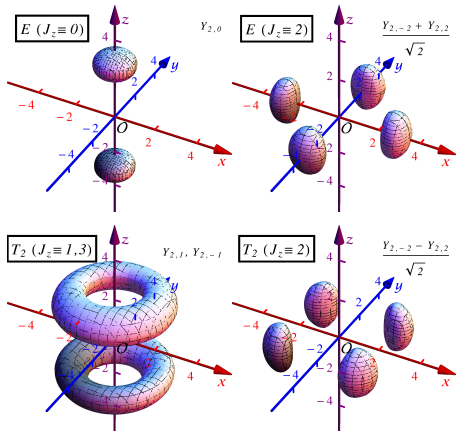


Cubic symmetry

Cubic symmetry group



Breaking of SO(3) rotational symmetry



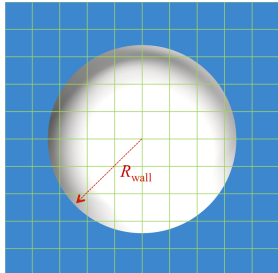
- In **the continuum**, rotational SO(3) symmetry is a strict symmetry.
- On a **lattice**, due to **lattice artifacts**, some orientations are **more energetically preferred**.

**irreducible representations of O group
(example: $J = 2$)**

	$J_z \pmod{4}$	Y_{LM}
A_1	0	Y_{00}
A_2	0, 1, 3	$(Y_{32} - Y_{3\bar{2}})/\sqrt{2}$
E	0, 2	$Y_{20}, (Y_{2\bar{2}} + Y_{22})/\sqrt{2}$
T_1	1, 2, 3	$Y_{10}, Y_{11}, Y_{1\bar{1}}$
T_2	2	$Y_{21}, (Y_{2\bar{2}} - Y_{22})/\sqrt{2}, Y_{2\bar{1}}$

Every **energy level J^π** split into several **irreps of cubic O group**

Spherical wall method



- Spherical wall method:

Place a hard wall at sufficiently large R

Energy spectrum \rightarrow phase shifts and mixings

$$\psi(r) \rightarrow [\cos \delta_L j_L(kr) - \sin \delta_L y_L(kr)]$$

$$\psi(R_{\text{Wall}}) = 0 \implies \tan \delta_L = \frac{j_L(kR_{\text{Wall}})}{y_L(kR_{\text{Wall}})}, k_i = \sqrt{2\mu E_i}$$

μ : reduced mass; E_i : energy spectrum

Borasoy et al., Eur. Phys. J. A 34(2007) 185

Carlson et al., Nucl. Phys. A 424 (1984) 47

- Easy to implement

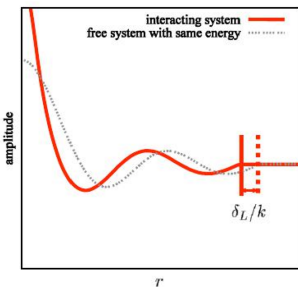
- Sensitive to energies, noisy;

- Less accurate for coupled channels:

- Only given one energy value E , to find three unknowns: $\delta_1, \delta_2, \varepsilon$

$$S = \begin{pmatrix} e^{2i\delta_1} \cos(2\varepsilon) & e^{i(\delta_1+\delta_2)} i \sin(2\varepsilon) \\ e^{i(\delta_1+\delta_2)} i \sin(2\varepsilon) & e^{2i\delta_2} \cos(2\varepsilon) \end{pmatrix}$$

- Have to use approximations

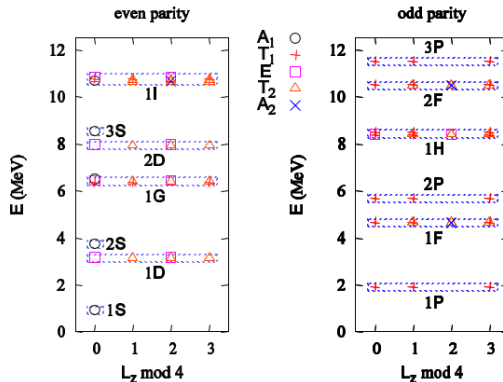


N-N energy levels on the lattice

Energy levels with hard spherical wall

$$R_{\text{wall}} = 10a$$

$$a = 1.97 \text{ fm}$$



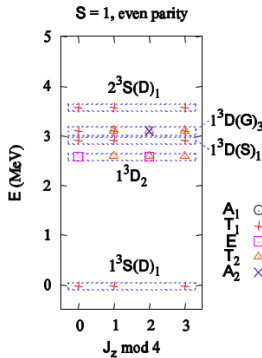
Energy shift from free-particle values gives the phase shift

N-N energy levels on the lattice

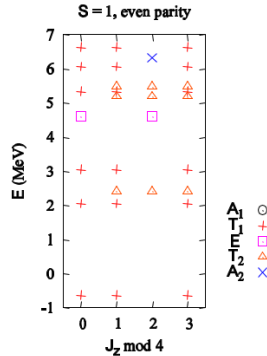
Comparison of spherical wall and periodic cube

Toy model: $V(\vec{r}) = C \left\{ 1 + \frac{r^2}{R_0^2} [3(\hat{r} \cdot \vec{\sigma}_1)(\hat{r} \cdot \vec{\sigma}_2) - \vec{\sigma}_1 \cdot \vec{\sigma}_2] \right\} \exp\left(-\frac{1}{2} \frac{r^2}{R_0^2}\right)$

Spherical wall, $R_{\text{wall}} = 10a$



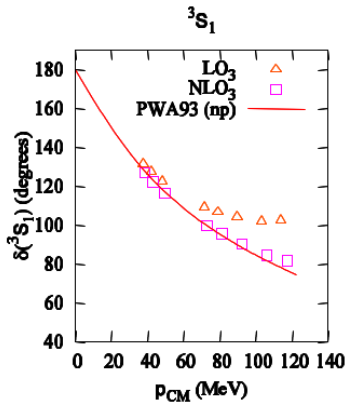
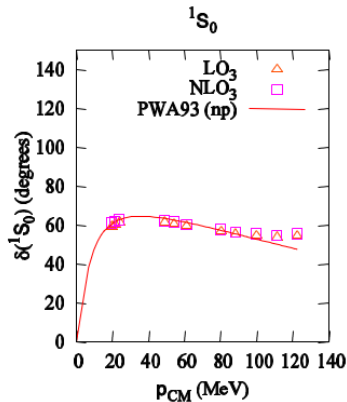
Periodic cube, $L = 12a$



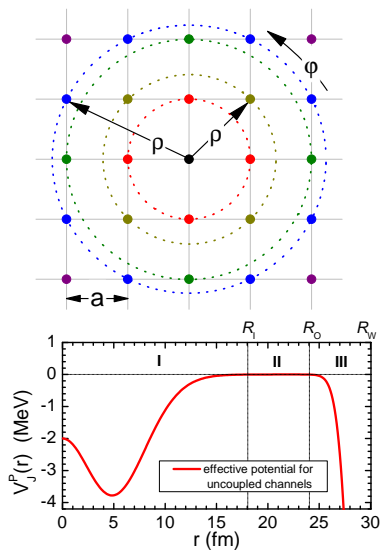
Nucleon-nucleon phase shifts

LO₃: S waves

$a = 1.97 \text{ fm}$

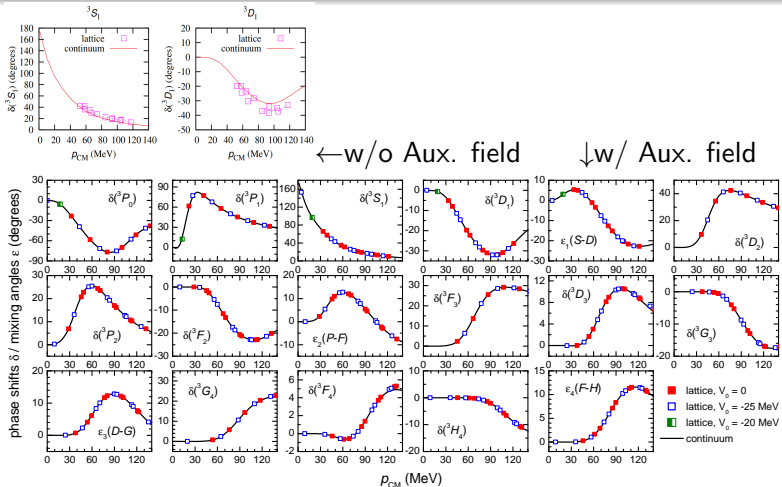


Auxiliary field method: Improved spherical wall method



- **Angular momentum projection:**
Expand wave functions on states with good angular momentum,
 $|\rho\rangle_{L,L_z} = \sum_r Y_{L,L_z}(\hat{r})\delta_{\rho,|r|}|r\rangle$
- **Auxiliary potentials:**
Twist wave functions at large R :
 $V_{\text{aux}} = V_0 \exp(-(r - R_{\text{Wall}})^2/a^2)$
shift V_0 to scan the continuum
- **For coupled channels:**
 $V_{\text{aux}} \rightarrow \begin{pmatrix} iU_{\text{aux}}(r) \\ -iU_{\text{aux}}(r) \end{pmatrix}$
Hermitian, but breaks time reversal
→ Kramer degeneracy
Two independent solutions for one E
- **Find phase shifts and mixings from asymptotic wave functions**
Lu et al., Phys. Lett. B 760 (2016) 309

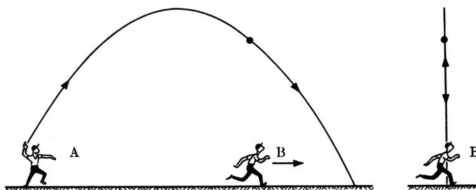
Auxiliary field method: Restoration of rotational symmetry



- Phase shifts and mixing angles for a tensor potential (toy model).
- $$V(r) = C \left\{ 1 + \frac{r^2}{R_0^2} [3(\hat{r} \cdot \sigma_1)(\hat{r} \cdot \sigma_2) - \sigma_1 \cdot \sigma_2] \right\} \exp \left(-\frac{r^2}{2R_0^2} \right)$$
- Continuum results by solving the Lippmann-Schwinger equation.
Lu et al., Phys. Lett. B 760 (2016) 309

Galilean invariance breaking

- For NN system, in center of mass frame $\mathbf{P}_{\text{c.m.}} = 0$, fit low-energy-constants to **Nijmegen Partial Wave Analysis**
- For 3N or more nucleons, nucleons might interact at $\mathbf{P}_{\text{c.m.}} \neq 0$.
- For **non-relativistic dynamics**, interaction should **NOT** depend on $\mathbf{P}_{\text{c.m.}}$. If not, we say there is a **Galilean invariance (GI) breaking**.
- A spatial lattice naturally breaks GI.
 - Lattice imposes momentum cutoff Λ on **single particle momenta** \mathbf{p}_1 and \mathbf{p}_2 , not the **relative momentum** $\mathbf{p} = (\mathbf{p}_1 - \mathbf{p}_2)/2$.
 - Lattice non-local operators (v -dependent) also break GI.
- GI should be restored before doing many-body calculations.



Restoration of Galilean invariance

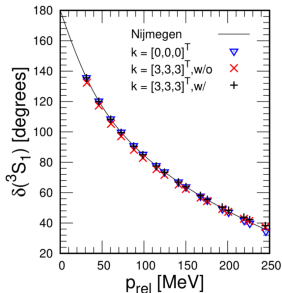
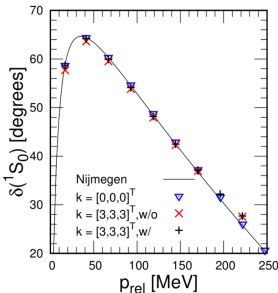
- Introduce counter term that **break the GI explicitly**,

$$V_{\text{GIR}} = C_{\text{GIR}} \sum_{\mathbf{n}} a_{\sigma}^{\dagger}(\mathbf{n}) a_{\rho}^{\dagger}(\mathbf{n}) \left[\sum_{\mathbf{m}}^{|m-n|=1} a_{\rho}(\mathbf{m}) a_{\sigma}(\mathbf{m}) - 6 a_{\rho}(\mathbf{n}) a_{\sigma}(\mathbf{n}) \right],$$

σ, ρ are spin/isospin indices.

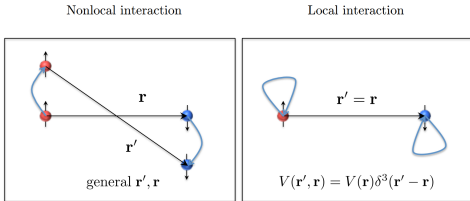
- In momentum space, $V_{\text{GIR}} \rightarrow -P_{\text{c.m.}}^2 + \mathcal{O}(P_{\text{c.m.}}^4)$
- Adjust parameter C_{GIR} to **absorb the GI breaking effects**.
- Test: compare **rest-frame** $\mathbf{k} = [0, 0, 0]$ with **moving frame** $\mathbf{k} = [3, 3, 3]$.

Li et al., Phys. Rev. C 99, 064001 (2019)



Local/non-local interactions

- General interaction $V(\mathbf{r}, \mathbf{r}')$
 - $\mathbf{r}' = \mathbf{r}$: Local interaction.
 - $\mathbf{r}' \neq \mathbf{r}$: Non-local interaction.



Example

- Two short-range interactions with the same strength C and range a :
$$V_1(\mathbf{r}, \mathbf{r}') = C \exp\left(-\frac{r^2}{2a^2}\right) \delta(\mathbf{r} - \mathbf{r}'), \quad V_2(\mathbf{r}, \mathbf{r}') = C \exp\left(-\frac{(r^2+r'^2)}{2a^2}\right).$$

V_1 is local, V_2 is non-local but separable.
- S-wave scattering amplitudes $f_1(p, p') = f_2(p, p')$ on the energy shell ($p = p'$).

V_1 and V_2 are equivalent in two-body sector (despite minor higher order corrections).

Is this still true in many-body sector?

Local/non-local interactions on the lattice

- On the lattice, the contact interactions are smeared to mimic the finite-range effects.
- Two types of smearing (\mathbf{n} denotes a lattice point):
 - Local smearing:

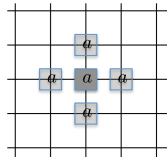
$$\rho_L(\mathbf{n}) = a^\dagger(\mathbf{n})a(\mathbf{n}) + s_L \sum_{\langle \mathbf{n}'\mathbf{n} \rangle} a^\dagger(\mathbf{n}')a(\mathbf{n}')$$

- Non-local smearing:

$$\rho_{NL}(\mathbf{n}) = a_{NL}^\dagger(\mathbf{n})a_{NL}(\mathbf{n}),$$

$$a_{NL}(\mathbf{n}) = a(\mathbf{n}) + s_{NL} \sum_{\langle \mathbf{n}'\mathbf{n} \rangle} a(\mathbf{n}').$$

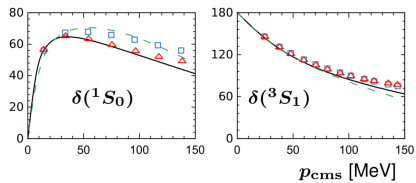
- The summation $\langle \mathbf{n}'\mathbf{n} \rangle$ includes all nearest-neighbouring lattice points.
- Different parameters s_L and s_{NL} give different locality.



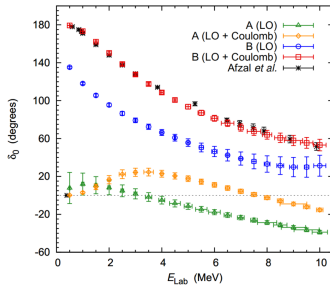
Elhatisari, Epelbaum, Krebs, Lahde, Lee, Li, BNL, Meissner, Rupak, PRL 119, 222505 (2017)

Effects of locality: NN and α - α scattering

- Both interaction A and B fitted to NN S-wave phase shift.
- A: Non-local; B: Local + non-local, also fitted to α - α phase shifts.



Nijmegen PWA —
Continuum LO - -
Lattice LO-A □
Lattice LO-B △



- Locality can only be probed by many-body calculations.
- What is the consequence for finite nuclei?

Effects of locality: finite nuclei

Ground state energies for α -like nuclei (in MeV):

Nucleus	A (LO)	B (LO)	A (LO + Coulomb)	B (LO + Coulomb)	Experiment
${}^8\text{Be}$	-58.61(14)	-59.73(6)	-56.51(14)	-57.29(7)	-56.591
${}^{12}\text{C}$	-88.2(3)	-95.0(5)	-84.0(3)	-89.9(5)	-92.162
${}^{16}\text{O}$	-117.5(6)	-135.4(7)	-110.5(6)	-126.0(7)	-127.619
${}^{20}\text{Ne}$	-148.0(1)	-178.0(1)	-137.0(1)	-164.0(1)	-160.645

- B (LO + Coulomb) reproduces the experiment (within 2% error).
- A (LO) describes a Bose condensate of particles:

$$E({}^8\text{Be})/E({}^4\text{He}) = 1.997(6) \quad E({}^8\text{Be})/E({}^4\text{He}) = 1.997(6)$$

$$E({}^{16}\text{O})/E({}^4\text{He}) = 4.00(2) \quad E({}^{20}\text{Ne})/E({}^4\text{He}) = 5.03(3)$$

Effects of locality: nuclear matter

- We define a one-parameter family of interactions with different locality:

$$V_\lambda = (1 - \lambda) V_\lambda + \lambda V_B,$$

λ quantifies the degree of locality.

$\lambda = 0$: completely non-local. $\lambda = 1$: locality fitted to α - α scattering.

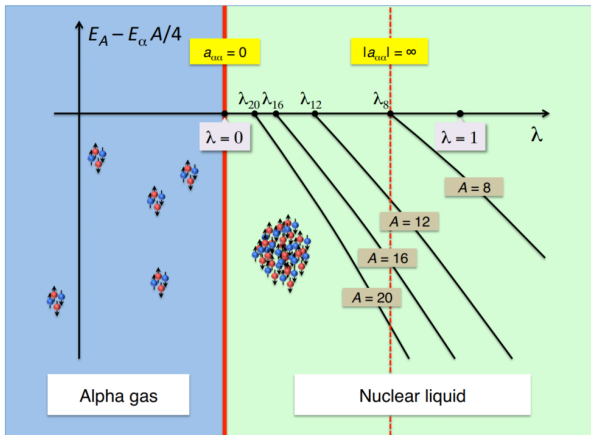
- The phase diagram of Symmetric Nuclear Matter (SNM) can be inferred from many-body simulations by switching off the Coulomb interaction.
- As a function of λ , there is a **quantum phase transition** at the point where the α - α scattering length $a_{\alpha\alpha}$ vanishes. [Stoff, Phys. Rev. A 49 \(1994\) 3824](#)
- It is a first-order transition from a Bose-condensed α -particle gas to a nuclear liquid.

Quantum Phase Transition

In physics, a quantum phase transition (QPT) is a phase transition between different quantum phases (phases of matter at zero temperature). Contrary to classical phase transitions, quantum phase transitions can only be accessed by varying a physical parameter—such as magnetic field or pressure—at absolute zero temperature. The transition describes an abrupt change in the ground state of a many-body system due to its quantum fluctuations.

Effects of locality: Zero-temperature phase diagram

$a_{\alpha\alpha}$: α - α scattering length. $E_A - E_\alpha A/4$: α -binding energy.
 $\lambda = 0$: purely non-local $\lambda = 1$: reality



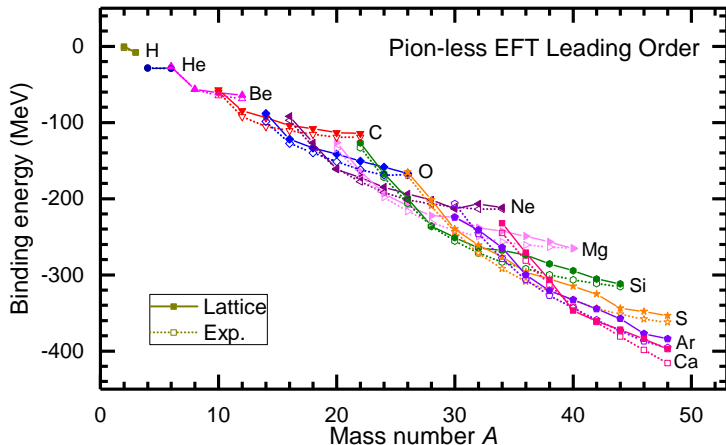
$$\begin{aligned}\lambda_8 &= 0.7(1) \\ \lambda_{12} &= 0.3(1) \\ \lambda_{16} &= 0.2(1) \\ \lambda_{20} &= 0.2(1) \\ \lambda_\infty &= 0.0(1)\end{aligned}$$

Elhatisari, Ning Li, Rokash, Alarcon, Du, Klein, B.L., Meißner, Epelbaum,
Krebs, Lähde, Lee, Rupak, [PRL 117 \(2016\) 132501](#)

Essential elements for nuclear binding

How many free parameters are essential for a proper nuclear force?

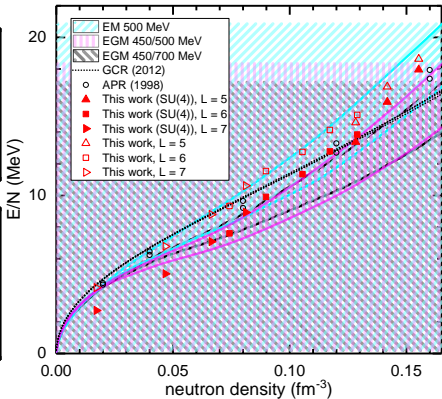
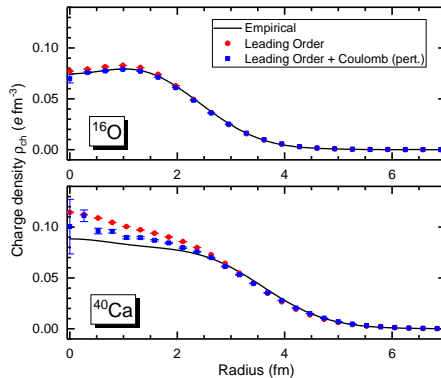
Answer: 4, Strength, Range, Three-body, Locality



B.L., Ning Li, Elhatisari, Lee, Epelbaum, Meißner, PLB 797, 134863 (2019)

Essential elements for nuclear binding

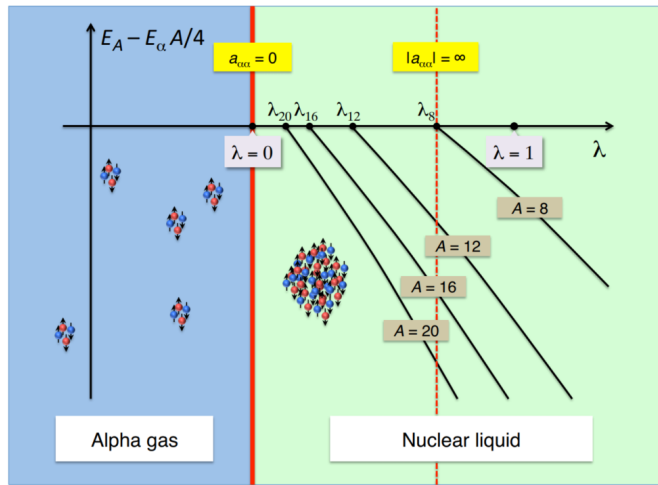
Charge density and neutron matter equation of state
are important in element creation, neutron star merger, etc.



B.L., Ning Li, Elhatisari, Lee, Epelbaum, Mei β nner, [PLB 797, 134863 \(2019\)](#)

Effects of locality: zero-temperature phase diagram

$a_{\alpha\alpha}$: α - α scattering length. $E_A - E_\alpha A/4$: α -binding energy.



$$\begin{aligned}\lambda_8 &= 0.7(1) \\ \lambda_{12} &= 0.3(1) \\ \lambda_{16} &= 0.2(1) \\ \lambda_{20} &= 0.2(1) \\ \lambda_\infty &= 0.0(1)\end{aligned}$$

Chiral nuclear force up to N³LO: lattice interactions

- We use a separable form $V \cong O^\dagger O$ for short-range interactions:

$$O_{S,L,J,J_z,I,I_z}^{2M,S_{NL}}(\mathbf{n}) = \sum_{S_z,L_z} \langle SS_z, LL_z | JJ_z \rangle \left[\psi(\mathbf{n}) \nabla_{1/2}^{2M} R_{L,L_z}^*(\nabla) \psi(\mathbf{n}) \right]_{S,S_z,I,I_z}^{S_{NL}}$$

$$R_{L,L_z}(\mathbf{r}) = \sqrt{\frac{4\pi}{2L+1}} r^L Y_{L,L_z}(\theta, \phi)$$

The indices in O and O^\dagger are all contracted to form scalars.

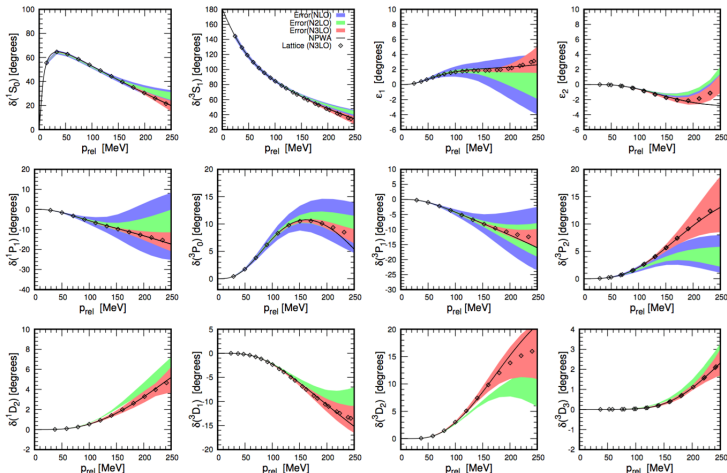
- Long-range interactions (1-pion, 2-pion) implemented using FFT:

$$V_{\text{OPE}} = -\frac{g_A^2}{8F_\pi^2} \sum_{\mathbf{n}', \mathbf{n}, S', S, I} : \rho_{S',I}(\mathbf{n}') f_{S'S}(\mathbf{n}' - \mathbf{n}) \rho_{S,I}(\mathbf{n}) :$$

$$f_{S'S}(\mathbf{n}' - \mathbf{n}) = \frac{1}{L^3} \sum_{\mathbf{q}} \frac{q_{S'} q_S \exp[-i\mathbf{q} \cdot (\mathbf{n}' - \mathbf{n}) - b_\pi(\mathbf{q}^2 + M_\pi^2)]}{\mathbf{q}^2 + M_\pi^2}$$

Ning Li, Elhatisari, Epelbaum, Lee, B.L., Meissner, [PRC 98, 044002 \(2018\)](#)

Chiral nuclear force up to N³LO: fit on the lattice



fit to N²LO: Alarcon, Du, Klein, Lahde, Lee, Ning Li, B.L., Luu, Meissner, EPJA 53, 83 (2017)

fit to N³LO: Ning Li, Elhatisari, Epelbaum, Lee, B.L., Meissner, PRC 98, 044002 (2018)

Center of mass problem and pinhole algorithm

Elhatisari, Epelbaum, Krebs, Lahde, Lee, Li, BNL, Meissner, Rupak, PRL 119, 222505 (2017)

Center of mass problem

- LEFT gives the eigen values of full many-body Hamiltonian H ,

$$|\Psi_{g.s.}\rangle \propto \lim_{\tau \rightarrow \infty} \exp(-\tau H) |\Psi_{\text{trial}}\rangle$$

- Translational invariance \implies Total momentum conservation

$$\Psi_{g.s.}(\mathbf{r}_1 + \mathbf{R}, \mathbf{r}_2 + \mathbf{R}, \dots, \mathbf{r}_A + \mathbf{R}) = \Psi_{g.s.}(\mathbf{r}_1, \mathbf{r}_2, \dots, \mathbf{r}_A)$$

- Measure densities in laboratory frame, $\rho(\mathbf{r}) = \sum_{N=1}^A \rho_N(\mathbf{r})$, Always get a uniform distribution $\rho(\mathbf{r}) = \text{Constant!}$
- Reason: nuclear structure information is contained in **A - 1 relative coordinates** $\mathbf{r}_2 - \mathbf{r}_1, \mathbf{r}_3 - \mathbf{r}_1, \dots, \mathbf{r}_A - \mathbf{r}_1$, not **A absolute coordinates** (relative to the lattice) $\mathbf{r}_1, \mathbf{r}_2, \dots, \mathbf{r}_A$.
- Solution: Expose the **internal structure** by removing the **redundant center of mass degree of freedom**
- Intrinsic** density distribution should be measured **relative to the center of mass** of all A nucleons,

$$\rho_{\text{c.m.}}(\mathbf{r}) = \sum_{N=1}^A \rho_N\left(\frac{1}{A} \sum_{N=1}^A \mathbf{r}_A + \mathbf{r}\right)$$

Pinhole algorithm

*Lattice EFT was unable to calculate observables in center of mass frame.
This can be solved by introducing the pinhole algorithm.*

Let $\rho_{i,j}(\mathbf{n})$ be the density operator for nucleons with spin i and isospin j at lattice site \mathbf{n} ,

$$\rho_{i,j}(\mathbf{n}) = a_{i,j}^\dagger(\mathbf{n}) a_{i,j}(\mathbf{n}),$$

we construct the normal-ordered A -body density operator

$$\rho_{i_1,j_1, \dots, i_A,j_A}(\mathbf{n}_1, \dots, \mathbf{n}_A) = : \rho_{i_1,j_1}(\mathbf{n}_1) \cdots \rho_{i_A,j_A}(\mathbf{n}_A) :$$

In the A -nucleon subspace, we note the completeness identity

$$\sum_{i_1,j_1, \dots, i_A,j_A} \sum_{\mathbf{n}_1, \dots, \mathbf{n}_A} \rho_{i_1,j_1, \dots, i_A,j_A}(\mathbf{n}_1, \dots, \mathbf{n}_A) = A!$$

Elhatisari, Epelbaum, Krebs, Lahde, Lee, Li, BNL, Meissner, Rupak, PRL 119, 222505 (2017)

Pinhole algorithm

In pinhole algorithm we work with the amplitude

$$\begin{aligned}& \mathcal{L}_{f,i}(i_1, j_1, \dots, i_A, j_A; \mathbf{n}_1, \dots, \mathbf{n}_A; L_t) \\&= \langle \Psi_f | M_*^{L'_t} M^{L_t/2} \rho_{i_1 j_1, \dots, i_A j_A}(\mathbf{n}_1, \dots, \mathbf{n}_A) M^{L_t/2} M_*^{L'_t} | \Psi_i \rangle.\end{aligned}$$

For $L_t \rightarrow \infty$ we get the ground state

$$M^{L_t/2} M_*^{L'_t} | \Psi_i \rangle \rightarrow \exp(-E_{g.s.} L_t/2) | \Psi_{g.s.} \rangle$$

and the probability distribution in the ground state is

$$|\Phi_{i_1 j_1, \dots, i_A j_A}^{\text{g.s.}}(\mathbf{n}_1, \dots, \mathbf{n}_A)|^2 = \frac{\langle \Psi_f | M_*^{L'_t} M^{L_t/2} \rho_{i_1 j_1, \dots, i_A j_A}(\mathbf{n}_1, \dots, \mathbf{n}_A) M^{L_t/2} M_*^{L'_t} | \Psi_i \rangle}{\langle \Psi_f | M_*^{L'_t} M^{L_t/2} M^{L_t/2} M_*^{L'_t} | \Psi_i \rangle}$$

When propagating, only the nucleons with the pinhole quantum numbers can pass!

Pinhole algorithm: Schematic

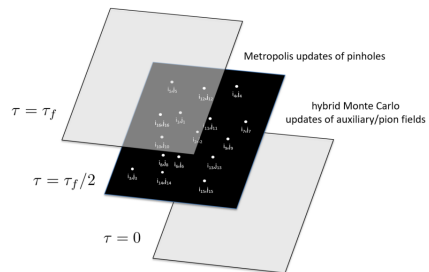
In terms of auxiliary fields, the amplitude Z can be written as a path-integral,

$$Z_{f,i}(i_1, j_1, \dots, i_A, j_A; \mathbf{n}_1, \dots, \mathbf{n}_A; L_t) \\ = \int \mathcal{D}s \mathcal{D}\pi \langle \Psi_f(s, \pi) | \rho_{i_1 j_1, \dots, i_A j_A}(\mathbf{n}_1, \dots, \mathbf{n}_A) | \Psi_i(s, \pi) \rangle.$$

We generate a combined probability distribution

$$P(s, \pi, i_1, j_1, \dots, i_A, j_A; \mathbf{n}_1, \dots, \mathbf{n}_A) = |\langle \Psi_f(s, \pi) | \rho_{i_1, j_1, \dots, i_A, j_A}(\mathbf{n}_1, \dots, \mathbf{n}_A) | \Psi_i(s, \pi) \rangle|$$

by updating both the auxiliary fields and the pinhole quantum numbers.



Observables in the intrinsic framework

Observables depending on the A -body probability distribution can be calculated now...

- Probability normalization:

$$\sum_{i_1, j_1, \dots, i_A, j_A} \sum_{\mathbf{n}_1, \dots, \mathbf{n}_A} |\Phi_{i_1, j_1, \dots, i_A, j_A}(\mathbf{n}_1, \dots, \mathbf{n}_A)|^2 = A!$$

- Nucleon density with respect to the center of mass:

$$\rho(\mathbf{n}) = \sum_{i_1, j_1, \dots, i_A, j_A} \sum_{\mathbf{n}_1, \dots, \mathbf{n}_A} |\Phi_{i_1, j_1, \dots, i_A, j_A}(\mathbf{n}_1, \dots, \mathbf{n}_A)|^2 \sum_{c=1}^A \delta(\mathbf{n}_c - \frac{1}{A} \sum_{s=1}^A \mathbf{n}_s - \mathbf{n})$$

- Probability of three spin \uparrow particles in a specific triangular shape:

$$\begin{aligned} \rho(d_1, d_2, d_3) &= \sum_{j_1, j_2, j_3} \sum_{\mathbf{n}_1, \mathbf{n}_2, \mathbf{n}_3} |\Phi_{\uparrow, j_1, \uparrow, j_2, \uparrow, j_3}(\mathbf{n}_1, \mathbf{n}_2, \mathbf{n}_3)|^2 \\ &\times \sum_{P(123)} \delta(|\mathbf{n}_1 - \mathbf{n}_2| - d_3) \delta(|\mathbf{n}_1 - \mathbf{n}_3| - d_2) \delta(|\mathbf{n}_2 - \mathbf{n}_3| - d_1), \end{aligned}$$

summation over all other indices and coordinates are omitted.

Pinhole algorithm: Intrinsic density distributions

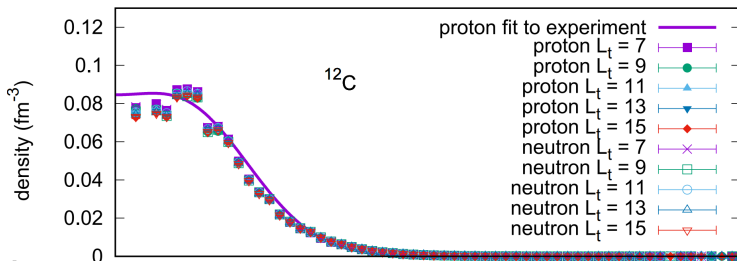
- Densities relative to the **center of mass**:

$$\rho_{\text{c.m.}}(r) = \sum_{n_1, \dots, n_A} |\Phi(n_1, \dots, n_A)|^2 \sum_{i=1}^A \delta(r - |r_i - R_{\text{c.m.}}|)$$

- First LEFT calculation of **nuclear intrinsic densities**.

- Proton radius** is included by **numerical convolution**

$$\rho(r) = \int \rho_{\text{Point}}(r') e^{-(r-r')/(2a^2)} d^3 r', \text{ proton radius } a \approx 0.84 \text{ fm.}$$

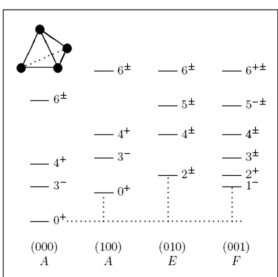


- Independent of projection time $L_t \iff$ In ground state

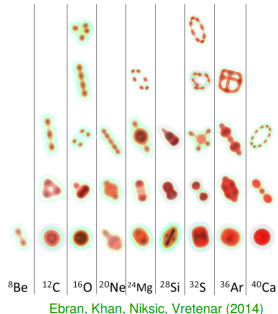
- Sign problem** suppressed \rightarrow Small errorbars

Elhatisari et al., Phys. Rev. Lett. 119, 222505 (2017)

Clustering in nuclei



Bijker, Iachello (2014)



Ebran, Khan, Niksic, Vretenar (2014)

- First introduced by Wheeler in 1937. [J. A. Wheeler, PR52-1083](#)
- Many works using density functionals, phenomenological models, et. al..
- Can we reproduce the clustering in ab initio calculations without assumption of their existence?

Measures of clustering

Short distance three- and four-nucleon operators serve as probes of the nuclear clusters,

$$\rho_3 =: \rho^3(\mathbf{n}) : /3!, \quad \rho_4 =: \rho^4(\mathbf{n}) : /4!,$$

ρ_3 and ρ_4 are independent of \mathbf{n} due to translational invariance. However, they might depend on the regularization scale (inverse lattice spacing in LEFT).

This dependence can be eliminated by considering the ratios $\rho_3(\Lambda)/\rho_{3,\alpha}(\Lambda)$ and $\rho_4(\Lambda)/\rho_{4,\alpha}(\Lambda)$, $\rho_{i,\alpha}(\Lambda)$ is the result for α particle in the same regularization scale Λ .

The remaining scale dependences are suppressed.

A model-independent way of quantifying clustering in nuclei!

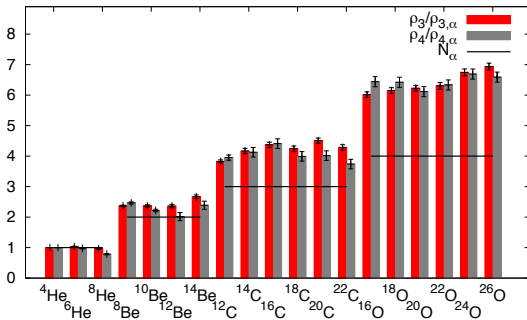
Measures of clustering

N_α is the naive estimate of the numbers of α -clusters from the proton numbers.

α -particles become more compact for larger $\frac{\rho_4}{\rho_{4,\alpha}} : \frac{\rho_3}{\rho_{3,\alpha}}$ ratio.

α -particles begin losing their identity when $\frac{\rho_4}{\rho_{4,\alpha}} - N_\alpha$ increases.

b

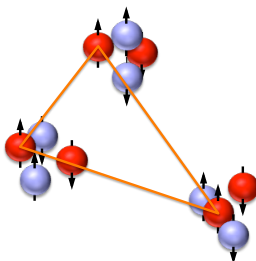


Elhatisari, Epelbaum, Krebs, Lahde, Lee, Li, BNL, Meissner, Rupak, PRL 119, 222505 (2017)

Triangles in carbon isotopes

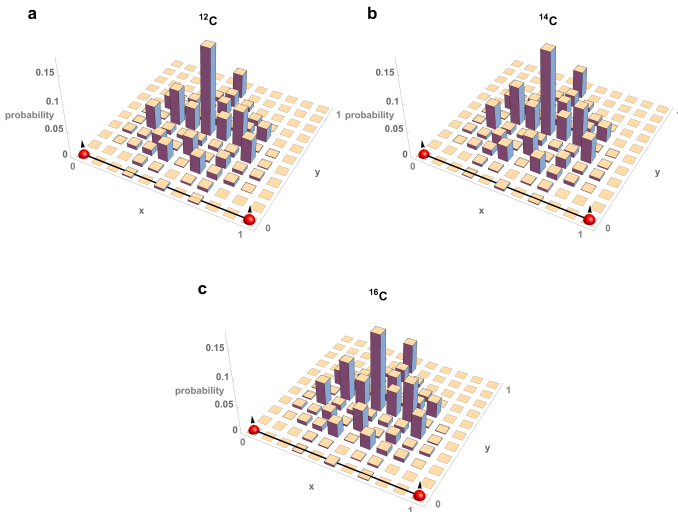
We always align the longest edge with the x -axis and keep the triangle in the x - y plane.

$$\rho(d_1, d_2, d_3) = \sum_{j_1, j_2, j_3} \sum_{\mathbf{n}_1, \mathbf{n}_2, \mathbf{n}_3} |\Phi_{\uparrow, j_1, \uparrow, j_2, \uparrow, j_3}(\mathbf{n}_1, \mathbf{n}_2, \mathbf{n}_3)|^2 \\ \times \sum_{P(123)} \delta(|\mathbf{n}_1 - \mathbf{n}_2| - d_3) \delta(|\mathbf{n}_1 - \mathbf{n}_3| - d_2) \delta(|\mathbf{n}_2 - \mathbf{n}_3| - d_1),$$



Elhatisari, Epelbaum, Krebs, Lahde, Lee, Li, BNL, Meissner, Rupak, PRL 119, 222505 (2017)

α -configurations along carbon isotopic chain



Elhatisari, Epelbaum, Krebs, Lahde, Lee, Li, Lu, Meissner, Rupak, PRL 119, 222505 (2017)

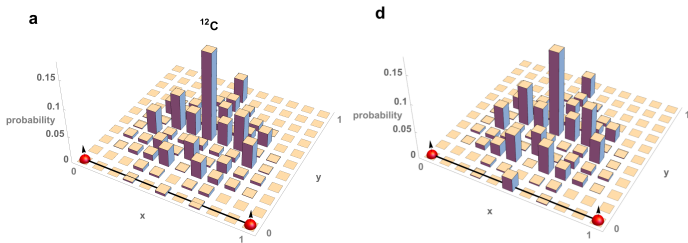
Toy model: Hard spheres in *s*-wave

We take the probability distribution (2.6 fm radius of ^{12}C , 1.7 fm radius of ^4He)

$$\exp \left[-\frac{\sum_i r_i^2}{2(2.6\text{fm})^2} \right] \prod_{j>k} \theta(|\mathbf{r}_j - \mathbf{r}_k| - 1.7\text{fm}),$$

the equivalent center-of-mass distribution is (4.5 fm average distance between α 's),

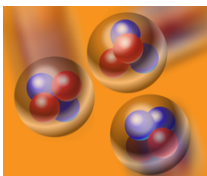
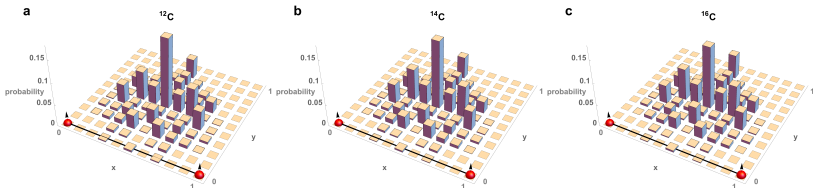
$$\prod_{j>k} \exp \left[-\frac{(\mathbf{r}_j - \mathbf{r}_k)^2}{2(4.5\text{fm})^2} \right] \theta(|\mathbf{r}_j - \mathbf{r}_k| - 1.7\text{fm}).$$



Elhatisari, Epelbaum, Krebs, Lahde, Lee, Li, Lu, Meissner, Rupak, PRL 119, 222505 (2017)

Pinhole algorithm: α -cluster geometry in carbon isotopes

Positions of 3rd proton relative to the other two in $^{12,14,16}\text{C}$

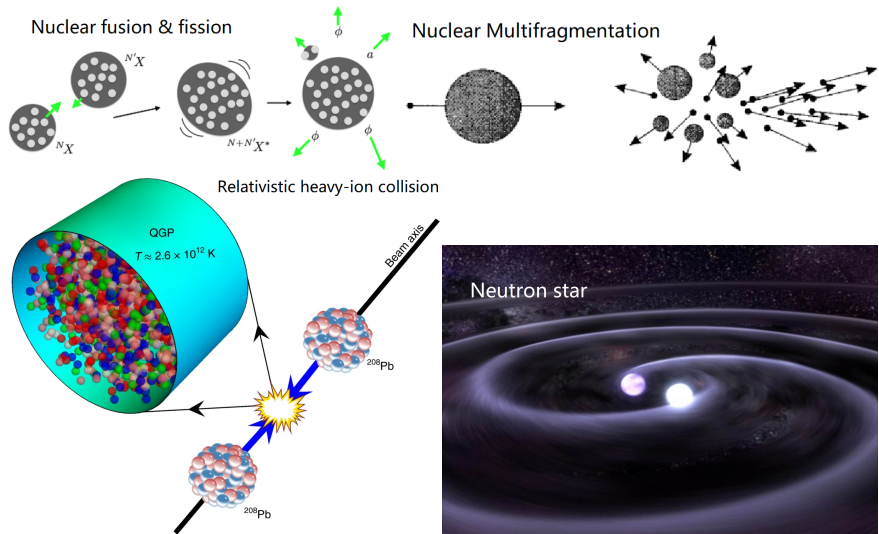


- **Hoyle state:** Triple- α resonance, essential for creating ^{12}C in stars (Hoyle, 1954). *Fine-tuning for life?* Epelbaum et al., Phys. Rev. Lett. 106, 192501 (2011)
- **Perspective:** important many-body correlations, understand **internal structures** of ground and excited states by *ab initio* calculations.
- **Next step:** high-precision chiral interaction → EM form factors, shape coexistence, clustering, ... Elhatisari et al., Phys. Rev. Lett. 119, 222505 (2017)

Ab initio nuclear thermodynamics

Bing-Nan Lu, Ning Li, Serdar Elhatisari, Dean Lee, Joaquín E. Drut, Timo A. Lähde, Evgeny Epelbaum, Ulf-G. Meißner,
[Phys. Rev. Lett. 125, 192502 \(2020\)](#).

How to heat up a nucleus



Microscopic picture of a hot nucleus

• Low excitation energies

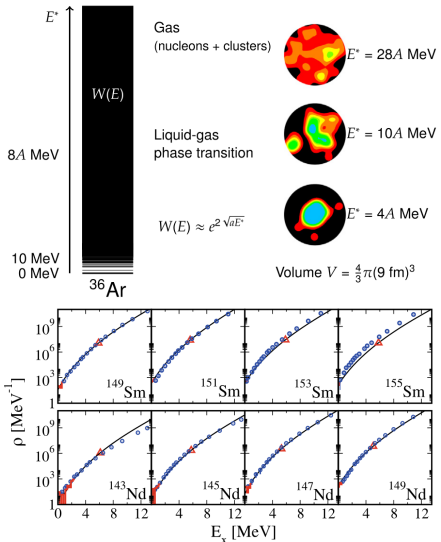
- Ground state, High spin, rotation, vibration, single particle motion, pairing, clustering...

• High excitation energies

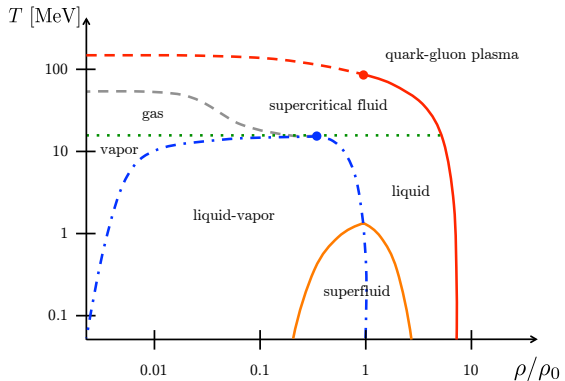
- Individual energy levels indistinguishable
- Level densities, temperature, pressure, chemical potential,...
- Evaporation, liquid-gas phase transition, multifragmentation,...

• Extremely high energies

- Hadron & quark degrees of freedom
- Quark-gluon plasma, quark deconfinement, ...



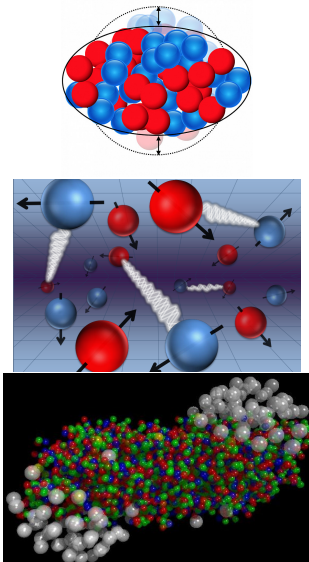
Nuclear phase diagram (theoretical)



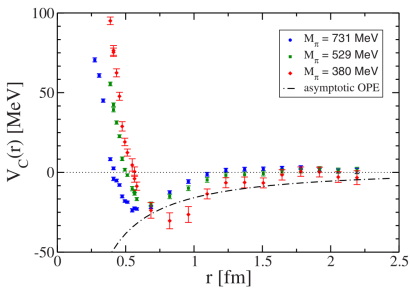
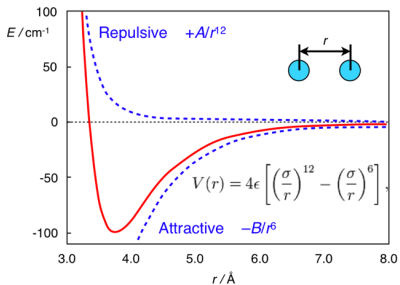
Strong interaction matter

Thermodynamic degrees of freedom:

Temperature, Density, Isospin, Hadronic,
Chemical potential, Pressure, etc...



Water molecule versus nucleons: similarity across orders



Upper: Van-der-Waals force between water molecules

- Strength $\sim 0.1 \text{ eV}$, range $\sim 1 \text{ \AA}$
- Phase transition at $T \sim 300 \text{ K} \sim 0.03 \text{ eV}$

Lower: Nucleon-nucleon potential from Lattice QCD

- Strength $\sim 10 \text{ MeV}$, range $\sim 1 \text{ fm}$
- What is the characteristic temperature?

Boltzmann constant
 $k \approx 10^{-4} \text{ eV/K} = 10^{-10} \text{ MeV/K}$
⇒ **Nuclear phase transition**
occurs at order $T \sim 10^{11} \text{ K}$

Response to external fields (light / neutrino)

Upper: Alcohol near T_c

- Critical Opalescence

Lower: Neutron star cooling

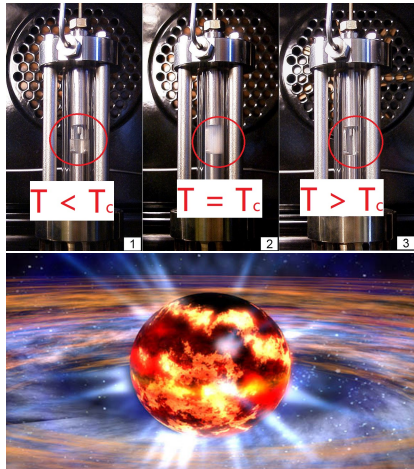
- Energies carried off by neutrinos
- Absorption by neutron matter

"In a newly born neutron star, neutrinos are temporarily trapped in the opaque stellar core, but they diffuse out in a matter of seconds, leaving most of their energy to heat the matter in the core to more than **500 billion kelvin**. Over the next million years, the star mainly cools by emitting more neutrinos."

PRL 120, 182701 (2018)

Lattice EFT simulation:

Ma, Yuan-zhuo et al., in preparation

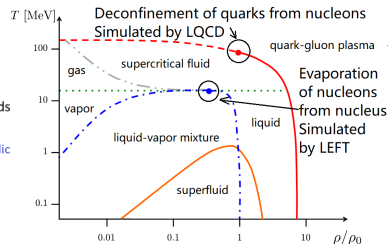
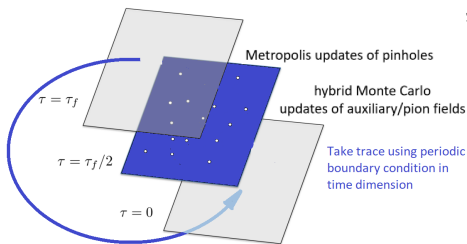


Simulate canonical ensemble with pinhole trace algorithm

- All we need: **partition function** $Z(T, V, A) = \sum_k \langle \exp(-\beta H) \rangle_k$, sum over all orthonormal states in Hilbert space $\mathcal{H}(V, A)$.
- The **basis states** $|n_1, n_2, \dots, n_A\rangle$ span the whole **A-body Hilbert space**. $n_i = (r_i, s_i \sigma_i)$ consists of **coordinate, spin, isospin** of i -th nucleon.
- **Canonical partition function** can be expressed in this **complete basis**:

$$Z_A = \text{Tr}_A [\exp(-\beta H)] = \sum_{n_1, \dots, n_A} \int \mathcal{D}s \mathcal{D}\pi \langle n_1, \dots, n_A | \exp[-\beta H(s, \pi)] | n_1, \dots, n_A \rangle$$

- **Pinhole algorithm** + **periodicity in β** = **Pinhole trace**
- Apply **twisted boundary condition** in 3 spatial dimensions to remove finite volume effects. Twist angle θ averaged with MC.



PRL 125, 192502 (2020)

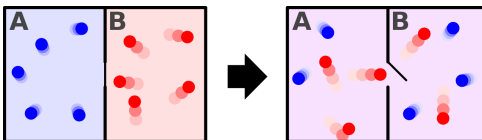
Reminder: Thermodynamics

- **Canonical ensemble:** free energy $F(T, V, A)$, partition function $Z = e^{-\beta F}$, closed system with fixed A .
- **Grand canonical ensemble:** thermodynamics potential $J(T, V, \mu) = F - \mu A$, open system with fixed μ .

Grand canonical ensemble simulation is conventional, however,

- Nuclear thermodynamics usually consider **small systems** $A \sim 10^2 - 10^3$.
- For **dilute system** $A \ll V$, not efficient, time complexity $\mathcal{O}(V^2)$.

Need a **canonical ensemble algorithm** for nuclear thermodynamics.

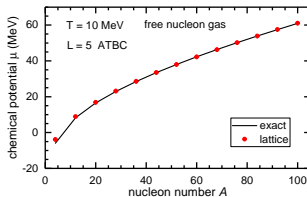
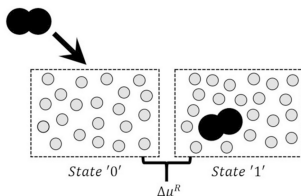


Extract intensive variables with Widom insertion method

- **Extensive variables:** Measured by operator insertion,
 - E.g., energy $E = \langle H \rangle_{\Omega}$, density correlation $G_{12} = \langle \rho(\mathbf{r}_1)\rho(\mathbf{r}_2) \rangle_{\Omega}$.
- **Intensive variables:** Measured by numerical derivatives,
 - E.g., pressure $p = -\frac{\partial F}{\partial V}$, chemical potential $\mu = -\frac{\partial F}{\partial A}$.
- **Widom insertion method:** Measure μ by inserting test particles (holes)
B. Widom, J. Chem. Phys. 39, 2808 (1963)

$$\mu = \frac{1}{2} [F(A+1) - F(A-1)] = \frac{T}{2} \ln \frac{Z_{A-1}}{Z_{A+1}} = \frac{T}{2} \ln \left[\frac{\sum_{1,2} \text{Tr}_A (\hat{a}_1^\dagger \hat{a}_2^\dagger e^{-\beta H} \hat{a}_1 \hat{a}_2) / (A-1)!}{\sum_{1,2} \text{Tr}_A (\hat{a}_1 \hat{a}_2 e^{-\beta H} \hat{a}_2^\dagger \hat{a}_1^\dagger) / (A+1)!} \right]$$

- **1, 2:** $L^3 \times 2 \times 2$ lattice sites, spins and isospins, sampled with **Monte Carlo**
- **($A \pm 1$)!:** **Combinatorial factors** for identical Fermions



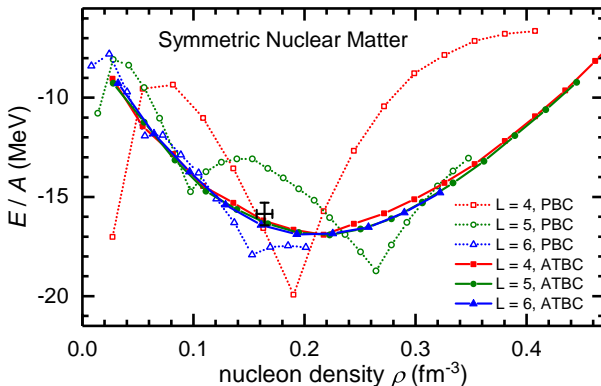
PRL 125, 192502 (2020)

Lattice interaction: Nuclear matter

PBC: Periodic Boundary Conditions: $\Psi(x+L) = \Psi(x)$

ATBC: Average Twisted Boundary Conditions: $\Psi(x+L) = e^{i\theta}\Psi(x)$

Averaging over θ 's' to remove fictitious shell effects

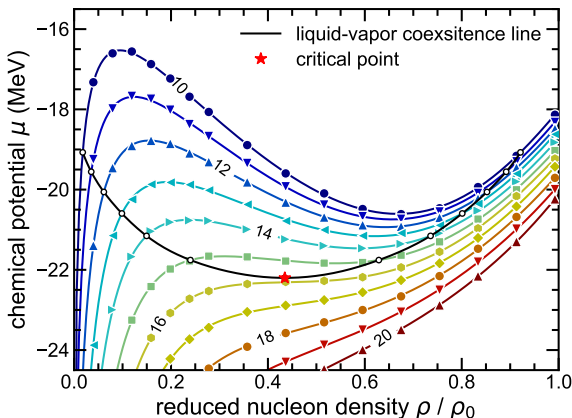


interaction from LU, et. al., Phys. Lett. B 797, 134863 (2019)
“Essential elements for nuclear binding”

Finite nuclear systems: Liquid-vapor coexistence line

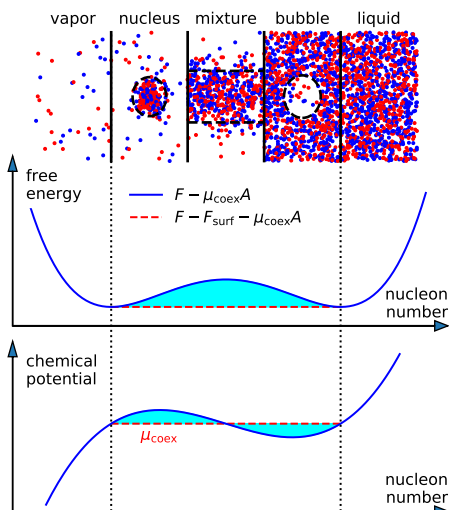
- First ***ab initio*** calculation of **nuclear liquid-gas phase transition**.
- Symmetric nuclear matter $N = Z$, lattice spacing $a = 1.32$ fm, volume $V = (6a)^3$, nucleon number $4 \leq A \leq 132$.
- Temperature $10 \text{ MeV} \leq T \leq 20 \text{ MeV}$, temporal step $\Delta\beta = 1/2000 \text{ MeV}^{-1}$.
- 288000 independent measurements for every data point.

Lu et al., Phys. Rev. Lett. 125, 192502 (2020)

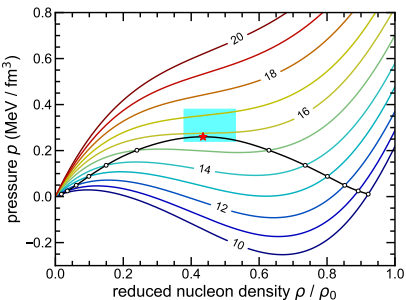


Finite nuclear systems: Surface effect

- The **backbending** in μ - ρ curves comes from the **surface effects**.
- Thermodynamic limit** ($A \rightarrow \infty$, $N \rightarrow \infty$), $\mu_{\text{liquid}} = \mu_{\text{vapor}} = \text{const.}$ at coexistence;
- Finite systems:** extra contribution of the **surface** to free energy F ;
- Surface area maximized at intermediate densities;
- $\mu = \partial F / \partial A$ exhibits a **backbending** at coexistence.



Critical point: Compare with experiment



Lu et al., Phys. Rev. Lett. 125, 192502 (2020)

- Pressure $p = \int \rho d\mu$ along every isotherm (Gibbs-Duhem equation).
- Extract T_c , P_c and ρ_c of neutral symmetric nuclear matter by numerical interpolation.
- Uncertainties estimated by adding noise and repeat the calculation.
- Experimental values and mean field results taken from Elliott et al., Phys. Rev. C 87, 054622 (2013)

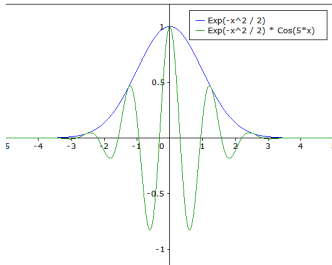
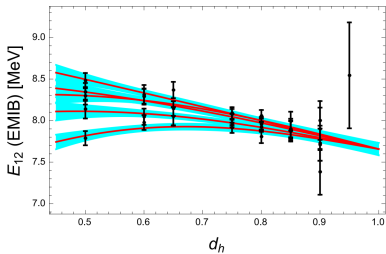
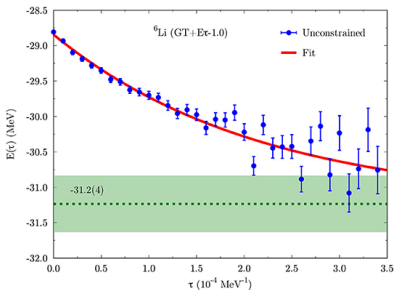
	This work	Exp.	RMF(NLSH)	RMF(NL3)
T_c (MeV)	15.80(3)	17.9(4)	15.96	14.64
P_c (MeV/fm ³)	0.260(3)	0.31(7)	0.26	0.2020
ρ_c (fm ⁻³)	0.089(1)	0.06(1)	0.0526	0.0463
ρ_0 (fm ⁻³)	0.205(0)	0.132		
ρ_c/ρ_0	0.43	0.45		

Lu et al., Phys. Rev. Lett. 125, 192502 (2020)

Perturbative Quantum Monte Carlo Method for Nuclear Physics

Bing-Nan Lu, Ning Li, Serdar Elhatisari, Yuan-Zhuo Ma, Dean Lee, Ulf-G.
Meißner,
Phys. Rev. Lett. 128, 242501 (2022).

Monte Carlo sign problem



- Sign problem: Monte Carlo works well for **well-behaved** functions, however, sometimes the integral becomes **highly oscillating**.
- QMC sign problem comes from the **fermion anti-symmetrization**.
- Split $H = H_0 + \lambda V_C$. H_0 : w/o sign problem; V_C : w/ sign problem.
- **Solution 1:** numerical extrapolation from $\lambda = 0$ to $\lambda = 1$.
- **Solution 2:** perturbative calculation near $\lambda = 0$.

Reyleigh-Schrödinger perturbation theory

For a Hamiltonian $H = H^{(0)} + \lambda V_C$,

- In conventional stationary perturbation theory:

$$E_i = E_i^{(0)} + \lambda \langle \Psi_i^{(0)} | V_C | \Psi_i^{(0)} \rangle + \lambda^2 \sum_{k \neq 0} \frac{\langle \Psi_k^{(0)} | V_C | \Psi_i^{(0)} \rangle}{E_k^{(0)} - E_i^{(0)}} + \mathcal{O}(\lambda^3)$$

$$|\Psi_i\rangle = |\Psi_i^{(0)}\rangle + \lambda \sum_{k \neq 0} \frac{\langle \Psi_k^{(0)} | V_C | \Psi_i^{(0)} \rangle}{E_k^{(0)} - E_i^{(0)}} |\Psi_k^{(0)}\rangle + \mathcal{O}(\lambda^2)$$

- However, in projection Monte Carlo algorithms,

$$E_{\text{g.s.}} = \lim_{\tau \rightarrow \infty} \exp(-\tau H) |\Psi_T\rangle$$

targets the ground states (or low-lying states) directly.

- In projection methods, excited states are very expensive. ← required for 2nd order energy or 1st order wave function!
- All projection QMC calculations use at most first order perturbation theory.

Perturbative Monte Carlo (ptQMC) algorithm

We can expand $|\Psi\rangle$ against V_C ,

$$|\Psi\rangle = \lim_{L_t \rightarrow \infty} M_0^{L_t/2} |\Psi_T\rangle = |\Psi_0\rangle + |\delta\Psi_1\rangle + \mathcal{O}(V_C^2), \quad (1)$$

with the wave functions defined as

$$|\Psi_0\rangle = \lim_{L_t \rightarrow \infty} M_0^{L_t/2} |\Psi_T\rangle, \quad |\delta\Psi_1\rangle = \lim_{L_t \rightarrow \infty} \sum_{k=1}^{L_t/2} M_0^{L_t/2-k} (M - M_0) M_0^{k-1} |\Psi_T\rangle,$$
$$E = E_0 + \delta E_1 + \delta E_2 + \mathcal{O}(V_C^3),$$

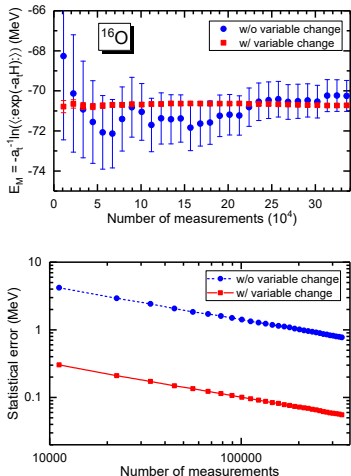
where the partial energy contributions at each orders are

$$\begin{aligned} E_0 &= \langle \Psi_0 | (K + V) | \Psi_0 \rangle / \langle \Psi_0 | \Psi_0 \rangle, \\ \delta E_1 &= \langle \Psi_0 | V_C | \Psi_0 \rangle / \langle \Psi_0 | \Psi_0 \rangle, \\ \delta E_2 &= (\langle \Psi_0 | V_C | \delta\Psi_1 \rangle - \delta E_1 \text{Re} \langle \delta\Psi_1 | \Psi_0 \rangle) / \langle \Psi_0 | \Psi_0 \rangle, \end{aligned} \quad (2)$$

in which all matrix elements and overlaps can be expressed with,

$$\begin{aligned} \mathcal{M}(O) &= \langle \Psi_T | M_0^{L_t/2} O M_0^{L_t/2} | \Psi_T \rangle, \\ \mathcal{M}_k(O) &= \langle \Psi_T | M_0^{L_t/2} O M_0^{L_t/2-k} M M_0^{k-1} | \Psi_T \rangle. \end{aligned}$$

ptQMC with realistic chiral interaction



Perturbed amplitude can be transformed into an approximate Gaussian integral with a variable change. Note that

$$\langle \exp(\sqrt{-a_t C} s p) \rangle_T \approx \exp(\sqrt{-a_t C} s \langle p \rangle_T)$$

$$\begin{aligned}\mathcal{M}_k(O) &= \langle \Psi_T | M_0^{L_t/2} O M_0^{L_t/2-k} M M_0^{k-1} | \Psi_T \rangle \\ &= \int \mathcal{D}c P(c + \bar{c}) \langle \cdots O \cdots M(s_k, c + \bar{c}) \cdots \rangle_T \\ &= \mathcal{M}(s) \exp\left(\frac{\bar{c}^2}{2}\right) \int \mathcal{D}c \exp\left(-\frac{c^2}{2} + \varepsilon\right)\end{aligned}$$

$$\bar{c}(n) = \left. \frac{\partial}{\partial c(n)} \ln \langle \cdots M(s_k, c) \cdots \rangle_T \right|_{c=0} \text{ is a constant field easy to calculate}$$

Integral over c calculated with MC

Left panel: Test calculation of the transfer matrix energy $E = -\ln(\langle \exp(-a_t H) \rangle)/a_t$
Lu et al., PRL 128, 242501 (2022)

Benchmark Hamiltonian: N²LO chiral Hamiltonian

We benchmark the ptQMC algorithm with a N²LO chiral Hamiltonian

$$H = K + V_{2N} + V_{3N} + V_{\text{cou}}$$

$$\begin{aligned}V_{2N} &= \left[B_1 + B_2(\boldsymbol{\sigma}_1 \cdot \boldsymbol{\sigma}_2) + C_1 q^2 + C_2 q^2(\boldsymbol{\tau}_1 \cdot \boldsymbol{\tau}_2) + C_3 q^2(\boldsymbol{\sigma}_1 \cdot \boldsymbol{\sigma}_2) + C_4 q^2(\boldsymbol{\sigma}_1 \cdot \boldsymbol{\sigma}_2)(\boldsymbol{\tau}_1 \cdot \boldsymbol{\tau}_2)\right. \\&\quad \left. + C_5 \frac{i}{2} (\mathbf{q} \times \mathbf{k}) \cdot (\boldsymbol{\sigma}_1 + \boldsymbol{\sigma}_2) + C_6 (\boldsymbol{\sigma}_1 \cdot \mathbf{q})(\boldsymbol{\sigma}_2 \cdot \mathbf{q}) + C_7 (\boldsymbol{\sigma}_1 \cdot \mathbf{q})(\boldsymbol{\sigma}_2 \cdot \mathbf{q})(\boldsymbol{\tau}_1 \cdot \boldsymbol{\tau}_2) \right] e^{-\sum_{i=1}^2 (p_i^6 + p_i'^6)/\Lambda^6} \\&\quad - \frac{g_A^2 f_\pi(q^2)}{4F_\pi^2} \left[\frac{(\boldsymbol{\sigma}_1 \cdot \mathbf{q})(\boldsymbol{\sigma}_2 \cdot \mathbf{q})}{q^2 + M_\pi^2} + C'_\pi \boldsymbol{\sigma}_1 \cdot \boldsymbol{\sigma}_2 \right] (\boldsymbol{\tau}_1 \cdot \boldsymbol{\tau}_2) \\V_{3N} &= \frac{c_E}{2F_\pi^4 \Lambda_\chi} e^{-\sum_{i=1}^3 (p_i^6 + p_i'^6)/\Lambda^6}\end{aligned}$$

with C_{1-7} , g_A , c_E etc. **low energy constants** fitted to N-N scattering or π -N scattering data, $\Lambda = 340$ MeV is the **momentum cutoff**

LEC	B_1	B_2	C_1	C_2	C_3
	-2.443	-0.125	0.143	-0.012	-0.013
LEC	C_4	C_5	C_6	C_7	c_E
	-0.020	0.273	0.0	-0.078	0.712

Table: Fitted LECs' in lattice unit

Zeroth order Hamiltonian (perturbative order)

We use a zeroth order lattice Hamiltonian that respects the Wigner-SU(4) symmetry

$$H_0 = K + \frac{1}{2} C_{\text{SU4}} \sum_{\mathbf{n}} : \tilde{\rho}^2(\mathbf{n}) :$$

The smeared density operator $\tilde{\rho}(\mathbf{n})$ is defined as

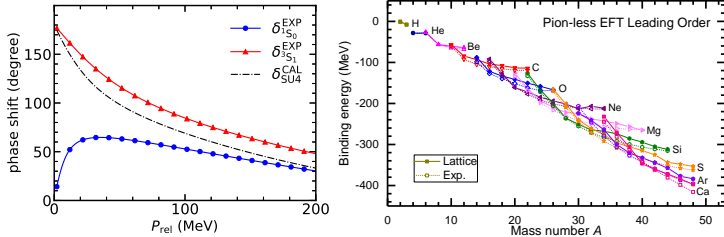
$$\tilde{\rho}(\mathbf{n}) = \sum_i \tilde{a}_i^\dagger(\mathbf{n}) \tilde{a}_i(\mathbf{n}) + s_L \sum_{|\mathbf{n}' - \mathbf{n}|=1} \sum_i \tilde{a}_i^\dagger(\mathbf{n}') \tilde{a}_i(\mathbf{n}'), \quad (3)$$

where i is the joint spin-isospin index

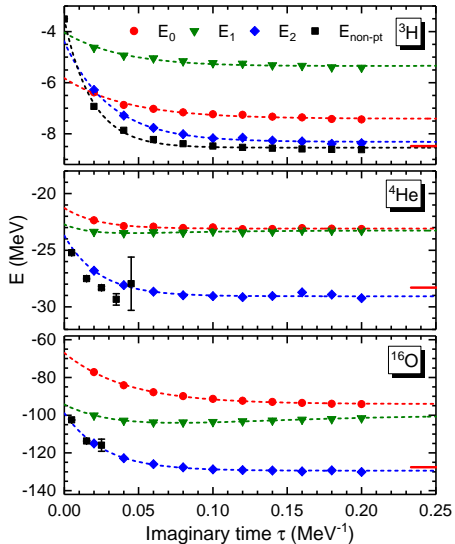
$$\tilde{a}_i(\mathbf{n}) = a_i(\mathbf{n}) + s_{NL} \sum_{|\mathbf{n}' - \mathbf{n}|=1} a_i(\mathbf{n}'). \quad (4)$$

In this work we use a lattice spacing $a = 1.32$ fm and the parameter set

$$C_{\text{SU4}} = -3.41 \times 10^{-7} \text{ MeV}^{-2}, s_L = 0.061 \text{ and } s_{NL} = 0.5.$$



Perturbative Monte Carlo with realistic chiral interaction

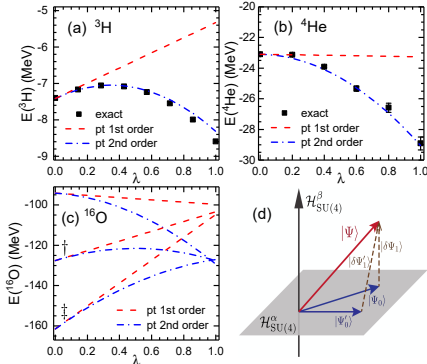


- We split $H = H_0 + (H - H_0)$ and perform perturbative calculations
- E_0 is the ground state of H_0
- $E_1 = E_0 + \delta E_1$ is the first order corrected energy
- $E_2 = E_1 + \delta E_2$ is the second order corrected energy
- $E_{\text{non-pt}}$ is the exact solution (\sim infinite order)
- Red bars on the right: Experiments
Lu et al., PRL 128, 242501 (2022)

For ^4He and ^{16}O , sign problem prevent us from going to large τ , resulting in large statistical errors. But no need to worry,

Perturbation theory can save us!

Abnormally large second order corrections



- Though consistent with the exact solutions, we found abnormally large second order energy corrections
- We write $H = H_0 + \lambda(H - H_0)$ and study the λ -dependence of energies ($0 \leq \lambda \leq 1$)
- $E_1 = E_0 + \lambda \delta E_1$ is a straight line
- $E_2 = E_1 + \lambda^2 \delta E_2$ is a parabola
- $E_{\text{non-pt}}$ is the exact solution
- For ${}^{16}\text{O}$ we use three different H_0
Lu et al., PRL 128, 242501 (2022)

As H_0 respects the $SU(4)$ symmetry, the wave function $|\Psi_0\rangle$ must belong to one of its irreducible representations (irreps). The full Hamiltonian H breaks the $SU(4)$ symmetry, thus its ground state $|\Psi\rangle$ is a mixture of different $SU(4)$ irreps. The components of $|\Psi\rangle$ that mixes the $SU(4)$ irreps can only be seen in $|\delta\Psi_1\rangle$ or δE_2

Reminder: A **symmetry breaking** perturbative Hamiltonian usually implies a large 2nd order energy correction!

Numerical results for several light nuclei

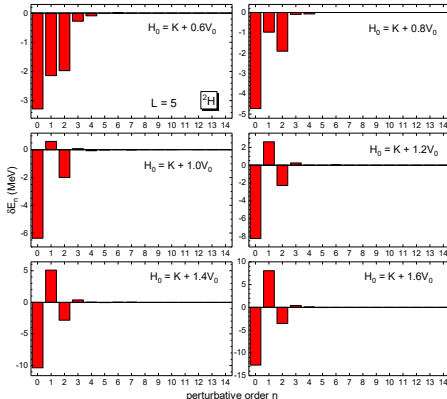
Table: The nuclear binding energies at different orders calculated with the ptQMC. E_{exp} is the experimental value. All energies are in MeV. We only show statistical errors from the MC simulations.

	E_0	δE_1	E_1	δE_2	E_2	E_{exp}
^3H	-7.41(3)	+2.08	-5.33(3)	-2.99	-8.32(3)	-8.48
^4He	-23.1(0)	-0.2	-23.3(0)	-5.8	-29.1(1)	-28.3
^8Be	-44.9(4)	-1.7	-46.6(4)	-11.1	-57.7(4)	-56.5
^{12}C	-68.3(4)	-1.8	-70.1(4)	-18.8	-88.9(3)	-92.2
^{16}O	-94.1(2)	-5.6	-99.7(2)	-29.7	-129.4(2)	-127.6
$^{16}\text{O}^\dagger$	-127.6(4)	+24.2	-103.4(4)	-24.3	-127.7(2)	-127.6
$^{16}\text{O}^\ddagger$	-161.5(1)	+56.8	-104.7(2)	-22.3	-127.0(2)	-127.6

Realistic N²LO chiral Hamiltonian fixed by few-body data + perturbative quantum MC simulation = nice agreement with the experiments

Excellent predictive power \Rightarrow Demonstration of both **nuclear force model** and **many-body algorithm**

Perturbative calculations beyond the second order



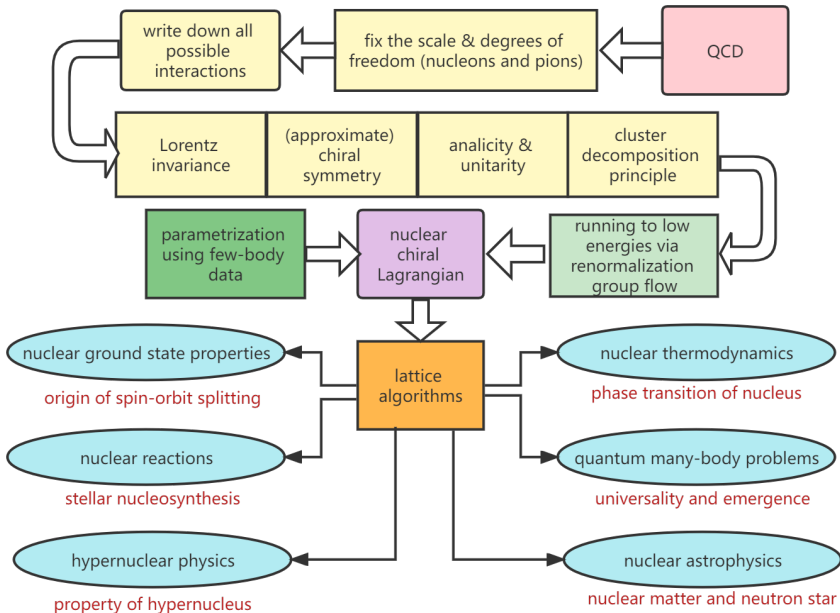
Perturbative energy correction δE_n of the deuteron at each order. For the zeroth order we show E_0 .

- We calculated deuteron energy $E(^2\text{H})$ in a small box $L = 6.6 \text{ fm}$ with a chiral Hamiltonian
- H is split as $H = (K + \mu V_0) + (V - \mu V_0)$, V_0 is the SU(4) interaction and V is the full chiral interaction
- $\mu = 0.6, \dots, 1.6$ is a constant

E_0 , δE_1 and δE_2 are always significant.
 δE_3 and higher order contributions are negligible, regardless of what H_0 we choose as the unperturbed Hamiltonian

The second order correction is large due to the symmetry breaking effect. There is no such mechanism for higher-order corrections, thus the higher-order corrections follow the usual power-counting hierarchy.

Summary



THANK YOU FOR YOUR
ATTENTION